SHAPE MEMORY ALLOY ROBOTIC TRUSS

Except where reference is made to the work of others, the work described in this thesis is my own or was done in collaboration with my advisory committee. This thesis does not include proprietary or classified information.

_____
Lori Michelle Prothero

Certificate of Approval:

_____   _____
Winfred A. Foster, Jr.   Robert S. Gross, Chair
Professor   Associate Professor
Aerospace Engineering   Aerospace Engineering

_____   _____
David A. Cicci   George T. Flowers
Professor   Dean
Aerospace Engineering   Graduate School

SHAPE MEMORY ALLOY ROBOTIC TRUSS

Lori Michelle Prothero

A Thesis

Submitted to the

Graduate Faculty of

Auburn University

in Partial Fulfillment of the

Requirements for the

Degree of

Master of Science

Auburn, Alabama
August 9, 2008

SHAPE MEMORY ALLOY ROBOTIC TRUSS

Lori Michelle Prothero

_____
Signature of Author

_____
Date of Graduation

VITA

Lori Michelle Prothero, daughter of Karen R. S. Prothero and granddaughter of the late Myrtle R. Setzer and the late Robert L. Setzer, was born November 4, 1981, in Jacksonville, Florida. She graduated as Valedictorian of Watauga High School in Boone, North Carolina, in June 2000. In May of 2004, Prothero graduated Cum Laude and as a University Honors Scholar with a Bachelor of Aerospace Engineering degree from Auburn University in Auburn, Alabama. During her first year at Auburn, Prothero began working in the Adaptive Aerostructures Laboratory for Dr. Ronald Barrett. In her third year of enrollment, she received the Auburn University Undergraduate Competitive Research Fellowship to independently research and develop a space structure utilizing adaptive materials. In April of 2004, Prothero presented her research findings at the National Conference of Undergraduate Research in Indianapolis, Indiana. In December of 2003 she was accepted to be a Master's candidate at Auburn University starting in the fall of 2004 to continue her work with adaptive structures. In the spring of 2006, Prothero's second generation prototype space truss using adaptive materials was tested in reduced gravity by the Auburn University NASA Reduced Gravity Student Team (Proposal ID: 2006-1767) in Houston, Texas aboard the NASA C-9 aircraft.

THESIS ABSTRACT

SHAPE MEMORY ALLOY ROBOTIC TRUSS

Lori Michelle Prothero

Master of Aerospace Engineering, August 9, 2008
(B.A.E., Auburn University, 2004)

113 Typed Pages

Directed by R. Steven Gross

The development, design, and analysis of a Shape Memory Alloy Robotic

Truss (SMART) actuator is presented in this research paper. SMART is a three-

degree of freedom actuator capable of large rotary and bending displacements using

shape memory alloy (SMA) wires as the mechanism for actuation. Using SMA

actuator wires instead of conventional hydraulic actuators simplifies the overall

complexity of design by reducing the number of working parts. SMA actuator wires,

because of vibrational dampening in the material itself, have a natural advantage over

hydraulic actuators because they are not susceptible to large parasitic vibrations and

long settling times inherent in hydraulic systems.

    With that said, the most radical development in the actuator design of SMART

is that the entire structure acts as an actuator instead of actuation occurring at only a

few synthetic joints. That is to say that the amount of actuation is dependent on the

length of SMART and corresponds directly to the structural stiffness of the truss.   For this reason, the truss backbone of the SMART actuator was designed to be structurally weak in torsion, strong in tension, and weak in axial bending to allow for the twisting and bending actuations. The actuation force is provided by the contraction of SMA wires which are attached in a specific pattern, to be described in further detail later, to wire guides at nodes along the truss. The force of the SMA wire's contraction is distributed to the truss through the nodes at which the SMA is attached. That is to say that the nodes connected to the SMA wire become closer, and as a result, the SMA's contraction actuates the entire truss.

The ability of the SMAs to contract is a unique material property of their crystalline structure to be trained at high heat to *remember* a desired length. When cold, SMAs can be mechanically stretched easily; however, they immediately return to the *remembered* length when a heat stimulus is applied. Exploiting this material property, electricity was supplied to one or multiple SMA wires in a simple circuit in which the SMA wires acted as the resistors.   The resistance produced heat in the SMA wires which then contracted in approximately a second to their remembered length. The result is that the entire truss actuated in a specified mode depending on which wires were heated.

Results of SMART from ground based testing and reduced gravity testing aboard the NASA C-9 aircraft, while undergoing parabolic trajectories to simulate reduced gravity, demonstrated the feasibility of SMART as an actuator truss capable of large actuations and functionality in a reduced gravity environment such as space.

ACKNOWLEDGEMENTS

Style manual or journal used: <u>American Institute of Aeronautics and Astronautics</u>

<u>Journal</u>

Computer software used: <u>Microsoft Word 2003, Microsoft Excel 2003</u>

TABLE OF CONTENTS

LIST OF SYMBOLS

SYMBOL	DEFINITION	UNITS
SMA	Shape Memory Alloy	
SMART	Shape Memory Alloy Robotic Truss	
NOL	Naval Ordnance Laboratory	
NiTiNOL	Nickel Titanium Alloy	
δ	Displacement, Elongation, or Deflection	in./deg.
ξ	Fraction of Phase Change from 0 to 1	none
T	Temperature	°C
A_S	Austenitic Phase Starting Temperature	°C
A_f	Austenitic Phase Final Temperature	°C
M_S	Martensitic Phase Starting Temperature	°C
M_f	Martensitic Phase Final Temperature	°C
®	Registered Trade Mark	
°C	Degrees Celsius	
DC	Direct Current	mV
Tan^{-1}	Inverse Tangent Function	
in. / ”	Inch	
° / deg	Degree	

V	Electrical Voltage
I	Electrical Current
R	Electrical Resistance
mV	Measure of Voltage, 10E-3 Volts
mA	Measure of Amperage, 10E-3 Ampere
sec	Unit of Time, Second
g	Unit of Mass, Gram
cm	Unit of Length, 10E-2 Meter
lb	Unit of Weight, Pound
μ	Micro-, 10E-6
Ω, ohm	Unit of Resistance
psi	Unit of Pressure/Modulus Unit, Pound Per Square Inch
GPa	Giga-Pascal, Unit of Stress (or Pressure), 10^9 Pascals
%	Part of Whole, Percent
cal	Unit of Heat, Calorie

LIST OF TABLES

LIST OF FIGURES

I. INTRODUCTION

Shape memory alloys (SMAs) are a special class of metals with a unique crystalline structure which can be heat trained to *remember* a specific size and shape to which it returns when a heat stimulus is applied. The unique characteristics of shape memory alloys (SMAs) were first discovered in the 1930s by Arne Örlander while he was working with Cadmium-gold alloys.[1] In 1962, William Buehler and other researchers at the Naval Ordnance Laboratory (NOL) discovered the memory effects in nickel-titanium alloy, which Buehler had previously renamed NiTiNOL in 1956 to include the Naval Ordnance Laboratory acronym.[2] Buehler discovered the ability of SMA to recover from high strains, of approximately 8% without plastic deformation.[2] Eight percent strain recovery means SMA can stretch as much as 8% of the original length and return to its original length without any permanent deformation or change in the strength of the SMA. Because of the ability to stretch and shrink repeatedly with strain recovery, SMA is the ideal material for mechanical devices which perform repetitive tasks.

There are three general categories of SMA devices: devices which use the SMA shape recovery directly, stress recovery devices which exploit the stress of SMA when it is constrained, and actuators which use the force induced by SMA to cause movements in other objects.[3]

An actuator, as the name implies, is a mechanical device which causes something else to move.[4] Actuators typically contain a large number of working parts such as gears and hydraulic pistons. SMA actuators reduce the complexity of conventional actuators by replacing the numerous mechanical parts with a single wire capable of the same actuation force.[5] Replacing hydraulic pistons and gears with a single wire also reduces the vibrational settling time, or shaking, as the actuator moves. Long vibrational settling times cause hydraulically mechanized machines to be more clumsy and imprecise in their movements.[4] As a result, vibration is a major limiting factor in robotic design which is highly dependent on precise actuators designed for specific desired movements.

There are already some SMA actuators for simple bending; however, only one of these designs by Padgett involves bending of an entire truss in two planes.[5] Howard, in his thesis on his design of a rotary SMA actuator, remarked that there exist very few designs for rotary actuators.[6] Howard's design is the only rotary design found of record which had more than one degree of freedom; however, both of its degrees of freedom are rotational and in a traditional joint-type actuator.[6] Drawing from the success of a bending-truss actuator by Padgett and the need for rotary actuators, the Shape Memory Alloy Robotic Truss was conceived as a two-degree-of-freedom bending actuator with a third rotary degree of freedom in the form of axial twisting of the truss for a total of three degrees of freedom.

Because the design of SMART was so complex, the final design was accomplished in a number of iterative stages with smaller, more specific goals. The first goal of this research project was to develop an axially twisting truss actuator as no

such device existed previously. The original hypothesis was that helically wound SMA wires around the truss when heated, would cause the entire truss to twist. After many design and prototyping iterations, a fully functional prototype twisting truss actuator was produced and tested. The twisting truss actuator will be discussed in further detail later in this thesis. After a twisting actuator had been developed, the second goal was to develop a bi-directional twisting actuator by incorporating opposing SMA actuator wires in a slightly modified truss. The Bi-directional requirement meant that the truss had to be untwisting mechanically rather than untwist due to cooling wire relaxation and gravity. After this second phase was accomplished, the truss had to be completely redesigned to accommodate bending. Even though the third generation truss design radically differed from the first two designs, the method by which the truss actuated was still the same as the first and second generations with the added bending capability similar to Padgett's actuator.

The third generation truss reverted to a configuration first proposed by Padgett for his bending truss actuator which had a common central spine. Along this spine were linearly spaced square trusses to which SMA attached linearly from truss to truss at each of the four corners; however, that is where the similarities between the Padgett design and SMART end. There are many key differences between the second and third generation designs as well as between the third generation bending and twisting actuator and Padgett's design.

In the third design generation, two actuators were incorporated into the same truss structure: one was a twisting actuator and the other was a bending actuator. By using the same truss for separate mode actuators, it was proposed that the truss could

be actuated as an integrated actuator of twisting and bending. This was also supported by a test in the first phase of design in which a linear set of SMA wires was connected at the same time while the twisting mode SMA wires were activated and did not have any affect on the actuation. In the third phase of design, small sliding insulators were added to the SMA wires in areas where the wires might have come into contact as a result of actuation of the bi-directional twisting. The effective use of insulators proved that SMA wires in bending could also be isolated from twisting-mode SMA wires through insulators as well. The fourth phase of the SMART project was extensive ground-based testing of both bending and twisting actuating trusses. The fifth phase was the reduced gravity test of the SMART bending mode and twisting mode aboard the NASA C-9 reduced gravity aircraft. The testing aboard the C-9 aircraft in parabolic freefall certified SMART and its structural components for reduced gravity operation such as found in space.

Further research is needed to develop a truly-integrated bending and twisting truss actuator as well as an actuator suitable for operation in a space environment.

II. SHAPE MEMORY ALLOY

Although Shape Memory Alloys were discovered much earlier by Arne
Orlander, they have only been used in engineering applications since the discovery of
NiTiNOL, nickel-titanium alloy, in the 1950's.[2] William Buehler discovered the shape
memory and high strain characteristics of NiTiNOL SMA quite by accident. In 1959,
Buehler and an assistant made six NiTiNOL bars in an arc-melting furnace. Buehler
dropped the first cooled bar on the concrete floor to see what the bar would do. The
bar made a thud indicative of some kind of vibrational damping within the material
itself. Buehler tested the other bars which were still warm and found the warm bars
resonated with a "bell-like quality sound." Buehler then cooled the warm bars in a
nearby water fountain to see if the resonance of the warm bars was temperature
dependent. He found that the bars made the same thud sound as the cooled bar did.
To test the reverse characteristic, he warmed the bars in boiling water, and the bars
regained their resonance.

Buehler continued to test the bars warm and cold and found the trend remained
the same; the warm bars were resonant and the cold bars were damped. Buehler
understood that the change in the acoustic damping indicated that the atomic structure
must change as a result of the temperature change. The significance of the change in

atomic structure at different temperatures was not significant until the shape memory effects of NiTiNOL were discovered.

Raymond Wiley joined the Naval Ordnance Laboratory (NOL) in 1960 and worked on failure analysis of different metals including NiTiNOL. In a briefing, Wiley demonstrated the fatigue resistance by repeatedly bending a NiTiNOL wire which had a diameter of one hundredth of an inch. Repeated bending typically weakens metals until they eventually break; however the NiTiNOL wire did not break. While passing the wire around the boardroom table so that everyone could have a turn bending the metal, David Muzzey, one of the technical directors of the NOL, "decided to see how it would behave under heat." Muzzey held the accordion folded NiTiNOL strip in the flame of his pipe lighter and the wire became instantly straight by itself. Buehler, hearing about the incident, decided the shape recovery phenomenon was related to the earlier observation about sonic damping and resonance; however, the shape memory effects would be more useful. Buehler's earlier observation that the structure of the NiTiNOL's atoms changed was later shown to be a change between two distinct crystalline structures depending on temperature.

2.1 CRYSTALLINE STRUCTURE

Shape memory alloys have two distinct phases called Austenite, which is the hot phase, and Martensite, which is the cold phase.[2] The Austenitic phase is known for its regular lattice pattern as shown in the following figure.[7]
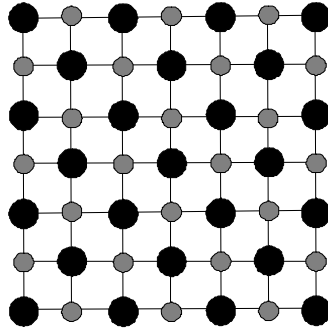
Figure 2.1.1 Austenitic (High Temperature) Crystal Structure.[2]

The darker, larger circles represent the Titanium metal ions and the lighter, smaller circles represent the Nickel metal ions. The pattern is repeated throughout the structure creating a regular face centered cubic crystal structure.[7] The Martensitic phase occurs as the Austenitic phase cools and becomes distorted as in the diagram below.[2]
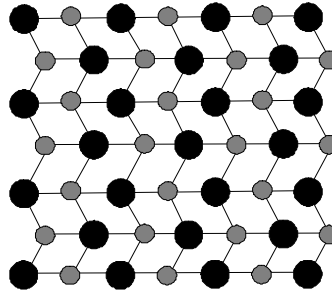
Figure 2.1.2 Martensitic (Cold Temperature) Crystal Structure.[2]

This type of alignment in which the crystals form parallelograms is called "monolithic."[7] The monolithic crystals align themselves as mirrored pairs called "twins." Twinning of the crystals does not affect the size or shape of the crystal significantly compared to the Austenitic lattice. As a stress or displacement is applied to the lattice, the crystalline structure becomes detwinned; however, the original monolithic crystalline structure remains as in Figure 2.1.3.
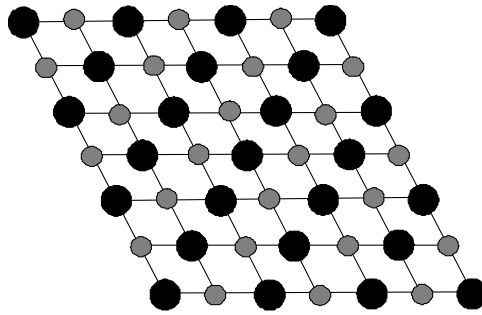
Figure 2.1.3 Deformed Martensitic (Cold Temperature) Crystal Structure.[2]

The structure shown in Figure 2.1.3, which is still in the Martensitic phase, has been deformed.[2] At this point heat can be applied and the lattice realigns in the Austenite form. The diagram below shows the crystalline transformations as the structure heats and cools.
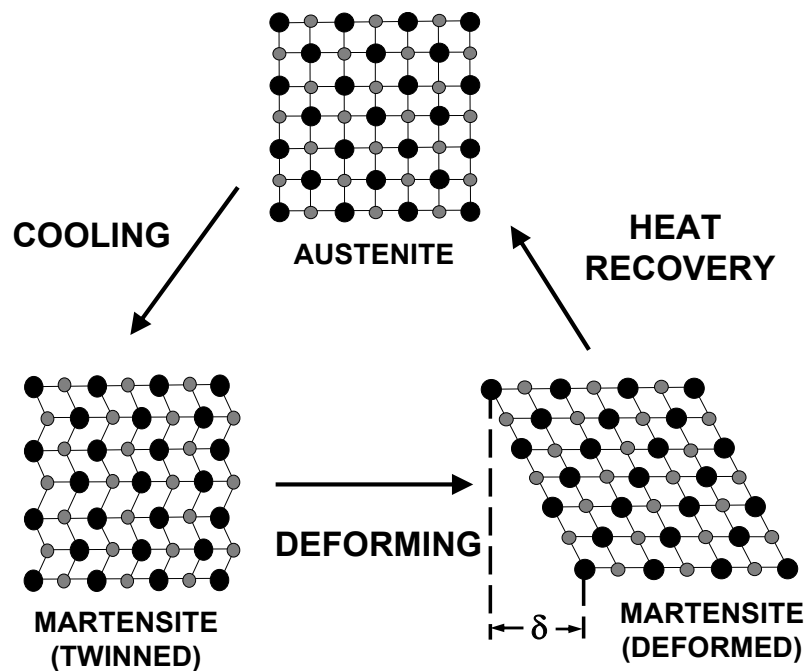
Figure 2.1.4 Diagram of Crystalline Transformations as
SMA Heats and Cools, δ Denotes Elongation.[2]

2.2 TEMPERATURE EFFECTS ON SHAPE MEMORY

The shape memory effect of shape memory alloys is directly related to the change in temperature of the SMA.[8] The figure below shows the change in phases as the metal cools or heats. The symbol ξ is the Martensite fraction and describes what state or fraction of phase transition the metal is in. The value for ξ is between zero
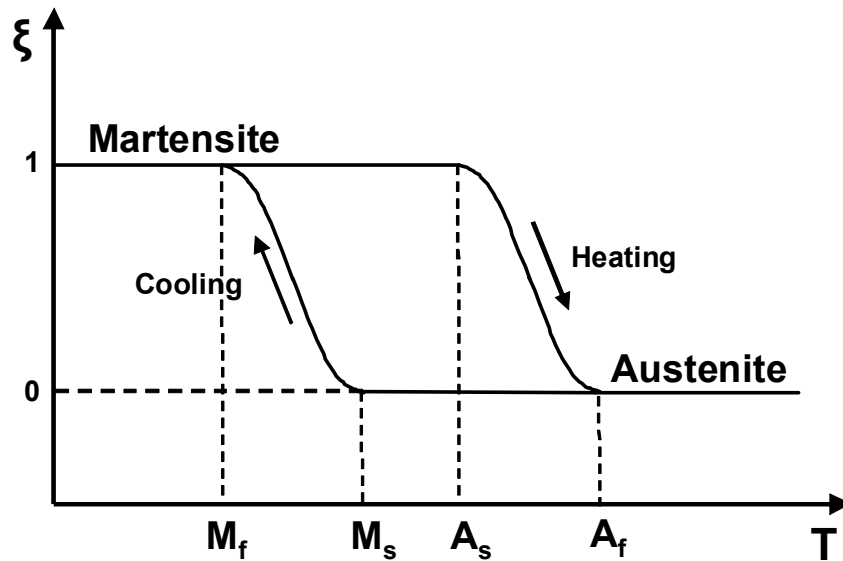
Figure 2.2.1 Phase Change Graph as a Function of Temperature.[4]

and one with zero denoting full Austenitic phase and one denoting full Martensitic phase. The symbol M_f represents the temperature at which and below which the full Martensitic phase is attained. The symbol M_s refers to the temperature at which the Martensitic phase begins. The symbol A_s corresponds to the temperature at which the Austenitic phase begins, and A_f is the temperature at which full Austenitic phase is achieved.

2.3 PHYSICAL SIGNIFICANCE

Recall in the Austenitic phase, the crystals align and *remember* a specific shape. As the material loses heat, it changes phases to the Martensitic phase which retains the same shape since twinning does not change the exterior shape significantly. As more heat is lost, the Shape Memory Alloy (SMA) becomes fully Martensitic, and it is possible to physically realign the crystals of the SMA. As the material is heated, it returns to the regular alignment of the Austenitic lattice without any trace of the Martensitic deformed shape.

$T = A_f$ **Austenitic, Initial State**

COOL

$T = M_f$ **Martensitic, Undeformed**

$T = M_f$ **Martensitic, Mechanically Deformed**

HEAT

$T = A_f$ **Austenitic, Shape Recovered**

HEAT   **COOL**

$T = M_f$ **Martensitic, Undeformed**
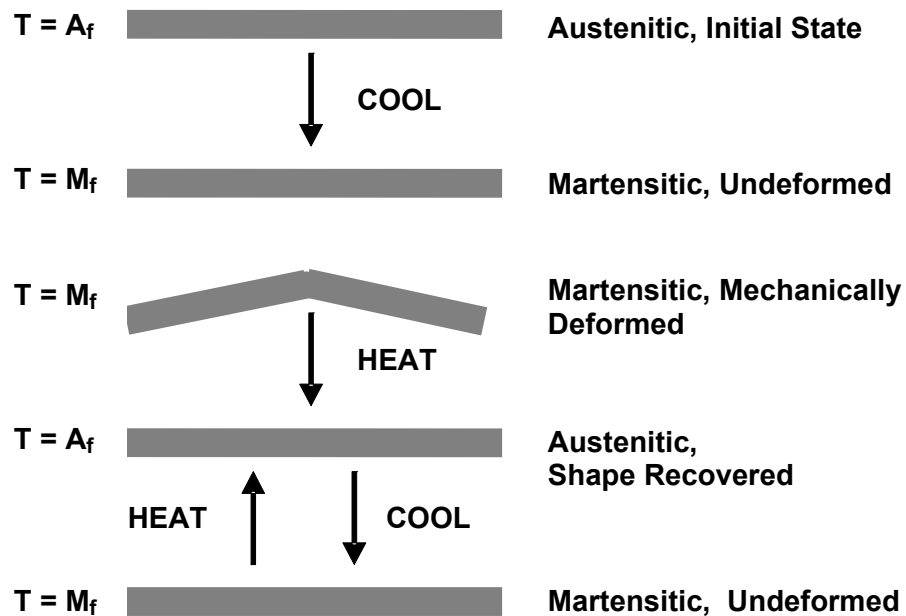
Figure 2.3.1 Diagram of Shape Memory Alloy Changing Physical Shape and Phases.[2]

The physical significance of the phase change can be seen in Figure 2.3.1. The warm Austenitic phase metal retains its shape as it cools to the Martensitic phase. In the Martensitic phase, the metal is deformed mechanically. As heat is applied, the metal returns to its original size and shape without any remaining deformation.

2.4 FLEXINOL®

      FLEXINOL® is the proprietary NiTiNOL alloy manufactured by Dynalloy, Incorporated and the particular NiTiNOL SMA wires used in SMART. [9] Dynalloy withholds the exact composition of FLEXINOL® as well as their processing and tempering of the alloy as trade secrets; however, they do supply extensive technical data specific to FLEXINOL® on their company website, www.dynalloy.com. According to the company website, this alloy was specifically engineered to be used in actuators; therefore, the company supplies the maximum pull force of a FLEXINOL® wire given its diameter. It is also assumed that in the typical application, the SMA wires will be heated by electrical resistance in a circuit. Dynalloy supplies the resistance of the wires in ohms per inch length as well as the current required in milliamps given the diameter of the wire in Table 2.4.[9]

Table 2.4 NiTiNOL Flexinol® Published Technical Data[9]

FLEXINOL© Technical Data						
Diameter Size (Inches)	Resistance (Ohms per Inch)	Maximum Pull Force (grams)	Current at Room Temperature (mA)	Contraction Time (seconds)	Off Time 70° C Wire (seconds)	Off Time 90° C Wire (seconds)
0.001	45	7	20	1	0.1	0.06
0.0015	21	17	30	1	0.25	0.09
0.002	12	35	50	1	0.3	0.1
0.003	5	80	100	1	0.5	0.2
0.004	3	150	180	1	0.8	0.4
0.005	1.8	230	250	1	1.6	0.9
0.006	1.3	330	400	1	2	1.2
0.008	0.8	590	610	1	3.5	2.2
0.01	0.5	930	1000	1	5.5	3.5
0.012	0.33	1250	1750	1	8	6
0.015	0.2	2000	2750	1	13	10
0.02	0.12	3562	4000	1	18	15

Using the resistance and current, it is easy to calculate the voltage across the wires given the circuit configuration. In a simple, one strand circuit with power supply connected directly to the wire, the voltage obeys Ohm's Law as presented in equation (1) with voltage, V, current, I, and resistance, R.

$$V = I \times R \qquad\qquad (1)$$

According to the supplied technical data as well as sample testing in the laboratory, FLEXINOL® has been shown to have very good fatigue qualities with the laboratory tested capability of over a hundred-thousand flex and relax cycles without breakdown.[4] FLEXINOL® is available in a range of gauges from 0.001 inch diameter to 0.02 inch diameter wires and has two different choices of transition temperatures: 70°C and 90°C.[9] The initial smaller scale prototype SMART used 0.001 inch diameter SMA wires; however, the final prototypes which were almost ten times larger in size than the original SMART switched to 0.005 inch diameter SMA wires since there was heavier structure to actuate in the later designs.

The contraction time is approximately one second for each of the wires with the relaxation time varying between 0.1 seconds to a few seconds due to the diameter and the transition temperature of the chosen wire.[9] The relaxation time varies because cooling is convective with ambient air and varies with surface area and thus with the diameter of the wire.[4] Crystalline differences in the transition temperature also cause the cooling times to be inherently different.[4] The technical data assumes that the wires are at room temperature and are isolated from radical air currents.[9]

12

The technical characteristics of FLEXINOL® samples were verified in the laboratory before selection for this project. The experiment used on a range of different gauge wires consisted of a simple weight, below the maximum pull strength of each wire, hanging from a single strand of SMA wire as shown in Figure 2.4.2.
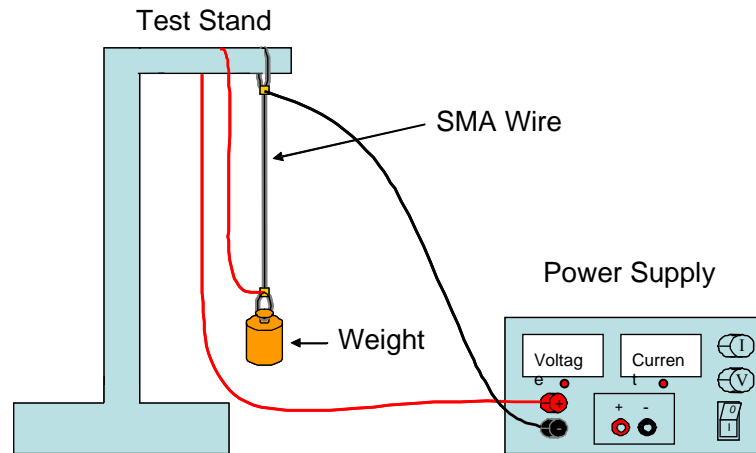
Figure 2.4.2 Simple Test of SMA Material Characteristics

An electrical circuit was made by attaching leads to crimps ten inches apart on the SMA wire suspending the weight. Note that the SMA did not carry the weight of the connecting lead wires; the bottom lead was draped across the test stand and the top was connected above the test section. The leads connected the SMA to the positive and negative terminals of a variable voltage and variable current power supply with built-in ammeter and voltmeter.

The voltage potential and current were slowly increased until the circuit was current limited, indicated by a red light on the power supply, at the desired test current. The voltage was increased until a spike was observed and that voltage was recorded. That voltage coincided with the moment at which the SMA lifted the weight. Due to the lag time in the reaction of the SMA of about one second, the

13

voltages were read directly from the power supply just as the ammeter registered the

voltage spike instead of using only the visual observation of the wire contracting. The

test was repeated with other incremental currents tested and corresponding voltages

recorded until the maximum current was exceeded and failure of the SMA occurred

due to overheating.

Figure 2.4.3 is the Voltage vs. Current test plot of a single strand of 0.01"

diameter SMA. The graph showed a clear linear relation with the slope of the linear

regression giving the resistance of the circuit according Ohm's Law. The wire's

theoretical resistance was calculated to be 5 ohms by multiplying the published

resistance of 0.5 ohms per inch times the length of 10 inches. The negligible increase

of 0.1 ohms resistance of the actual circuit was due to the brass crimps, connecting

wires, and resistance in the power supply with internal ammeter and voltmeter.

Testing of different diameter wires with the same test circuit also had an increase of

0.1 ohms which was determined to be a constant of the testing circuit.
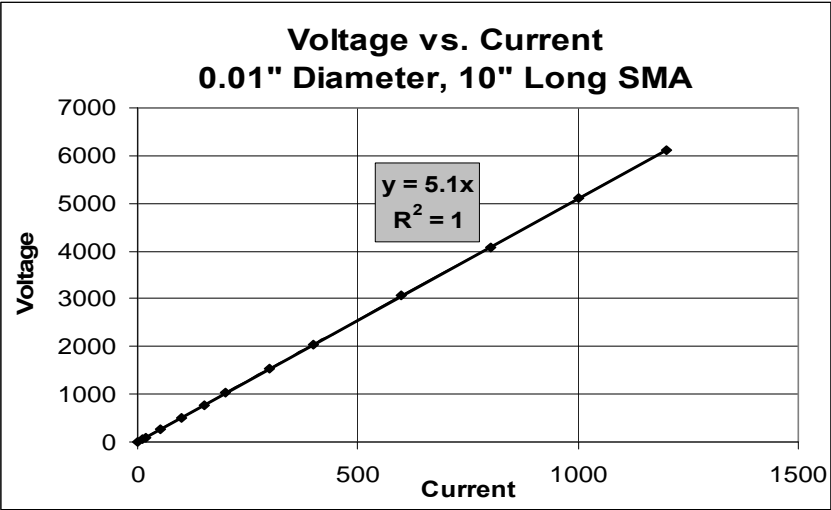
Figure 2.4.3. Sample Test Data from Material Test of a 0.01" Diameter SMA Wire

14

III. INITIAL DESIGN PHASE

The first challenge was to establish the initial and derived requirements of the design. To create a twisting only actuator, the truss had to be structurally flexible in torsion while stiff in tension and compression. The truss also had to accommodate connections and wire guides for the SMA to transfer force from the SMA as torque on the truss. The SMA wires, which were heated by electricity, had to be attached in such a way that the wires would not touch each other or anything that would conduct electricity.

3.1 STRUCTURAL DESIGN

The first requirement that the truss has to be flexible in torsion and stiff in tension and compression imposed that the truss be fixed in five of the six degrees of freedom: translation in the x-, y-, and z-direction and rotation about the x-, y-axis, while still being able to rotate easily about the z-axis as shown in Figure 3.1.1.

Triangular trusses were used to constrain the xy-plane of the truss, which constrained translations in the x- and y-directions. Stiff horizontal beam members connect the vertex of one triangular truss to the corresponding vertex of another as in Figure 3.1.1. The arrangement of the three horizontal beams with a triangular base effectively constrained bending in the xz- and yz- planes as well as any linear

translations along the z-axis. Because the horizontal beams were perpendicular to the triangular trusses, this left the 3-D structure unconstrained in twisting about the z-axis since force carried in the horizontal beams were out of the xy-plane.
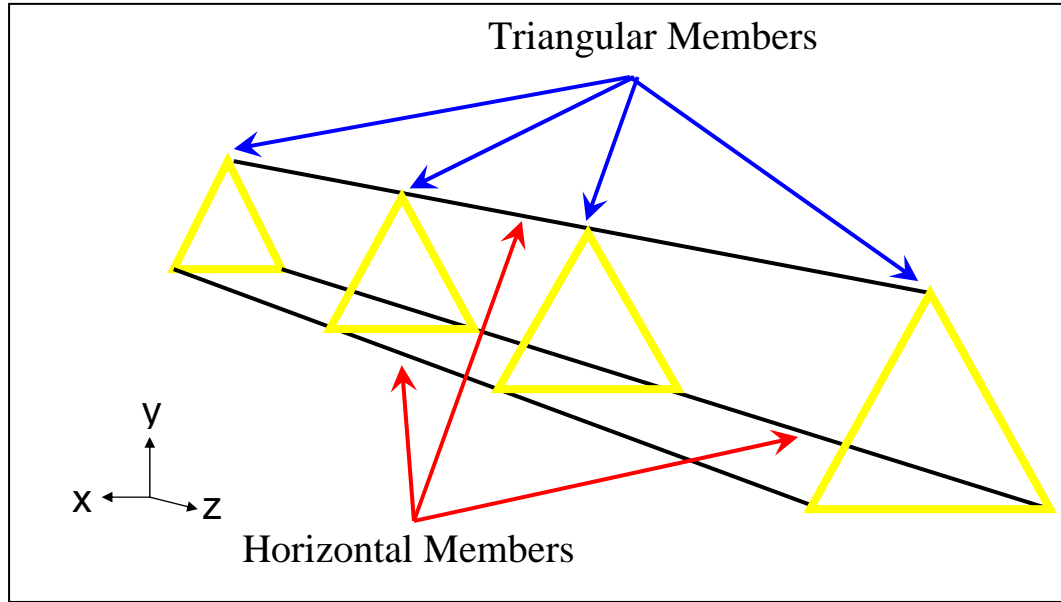
Figure 3.1.1 Shape Memory Alloy Truss Schematic with Coordinate Axes.

The joints between the triangular trusses and the horizontal beams had to withstand high stresses. To constrain local rotations about the x- and y-axis, the joints between the triangle trusses and the horizontal members had to be reinforced with high shear strength epoxy. The length of the horizontal members between triangular trusses also affected the strength of the truss. Adding more triangular trusses and moving them closer together resulted in stiffening the structure but reduced twisting flexibility. Conversely, reducing the distance between triangular trusses and thus reducing the number of trusses along the horizontal beams decreased structural stiffness and increased twisting flexibility. After several sample configurations were tested, the spacing between triangular trusses was sized appropriately to provide a stably

stiffened structure which retained the a maximum amount of flexibility. The

triangular trusses which measure one inch on each side, were spaced every two inches

along the horizontal beams.

3.2 MATERIAL SELECTION

Materials were carefully chosen for the truss members. Boron filaments

which were 0.050 inch diameter were selected for the horizontal members because of

their high compressive strength. Boron has a Young's modulus of elasticity of 478

GPa.[10] Compared to the Young's modulus of elasticity of steel, which is 200 GPa,[11]

boron is more than twice as stiff as steel.

Strands of prepreg KEVLAR® which measured 0.04 inches by 0.012 inches

were selected to make the triangular truss members. KEVLAR® possesses very good

tensile stiffness and strength properties while being poorer in compression. Due to

twisting actuation of the truss, the KEVLAR® trusses were only subjected to high

tension loads such that given the scale of the application, the local stiffness of the resin

in the KEVLAR® truss was sufficient for the nominal compressive loads. The

modulus of elasticity of KEVLAR® is 60 – 120 GPa and the tensile strength is 3 GPa,

or 3000 MPa.[12]

Incorporating the SMA actuation into the truss posed some difficulty. To

actuate the truss, the SMA needed to be attached to the truss to transfer the pull force

evenly at each node. The main obstacle was that SMA is difficult to bond with any

material, including with itself, because the elasticity and strain recovery that make the

material so useful, also prevents gluing, soldering, compression fitting, etc.

Many methods were tested before discovering that the most effective method for constraining SMA is to knot it with itself inside of a crimp. The friction of the knot and crimp was sufficient to hold the SMA since the force required to pull the SMA out of it is usually more than the maximum load rated for the wire. It was simply not practical to replicate the complicated knot/crimp joint while ensuring even pre-tensioning between each crimped section of SMA at each of the three nodes of all the triangular trusses. As a result, wire guides were incorporated into the KEVLAR® trusses through with the SMA could transfer the load as a contact load. The SMA wires at each end of the truss were knotted and crimped with a crimp larger that the diameter of the wire guide so that it could not be pulled through the hole.

Another concurrent complication in the design was that the SMA wires had to be electrically insulated from each other as well as from the boron filaments which are conductors. Incorporating the wire guides into the triangular trusses was the logical solution since KEVLAR® is an electrical insulator. SMA wire guides with a diameter of 0.01 inch were added at each node of the KEVLAR® triangle design with a geometric arrangement which prevented the SMA wires from touching each other or the boron.

3.3 KEVLAR® TRUSS MANUFACTURING

A single strand of KEVLAR® prepreg was tied in a pattern of knots, molded around piano wires larger than the diameter of the horizontal members, and pressed between two metal caul plates to create a triangular truss with holes large enough to accept the boron filaments at each vertex as well as the SMA as shown in Figure 3.3.1.
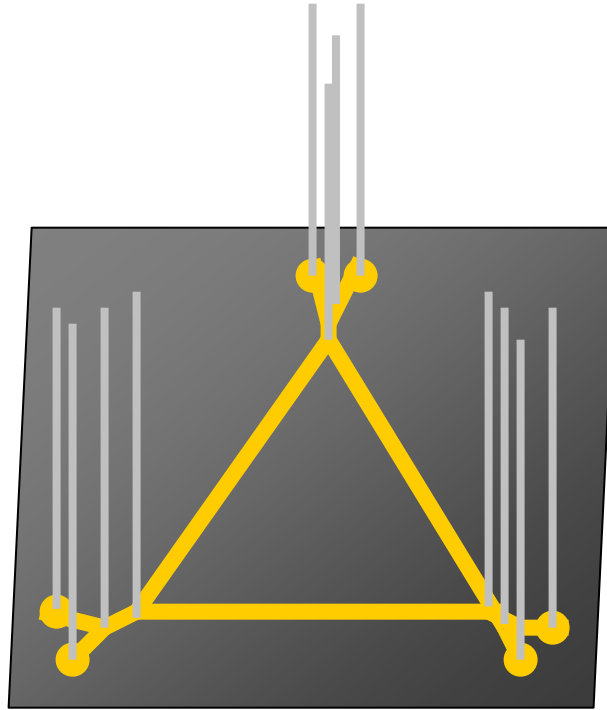
Figure 3.3.1 Schematic of a KEVLAR® Truss Lay-Up

Whole stacks of molded KEVLAR® using the top caul-plate surface as the

bottom surface for the next mold were stacked together and clamped. This method of

efficient manufacturing was developed by Padget; however, adding knots and weaving

the strands for added strength and adhesion of the epoxy was unique to this particular

application. The whole stack was placed in an autoclave to cure the impregnated resin

in the KEVLAR® strand. The KEVLAR® triangles were heated in the autoclave for

eight hours at 170°C using standard composite materials manufacturing techniques.

The result of the process can be seen in Figure 3.3.2 and Figure 3.3.3 which depict the

regular pattern of the finished KEVLAR® triangular truss. The wire guides were

positioned symmetrically at each vertex of the triangular truss. Figure 3.3.2 shows the

indexing system of holes in the triangular truss sections.

19
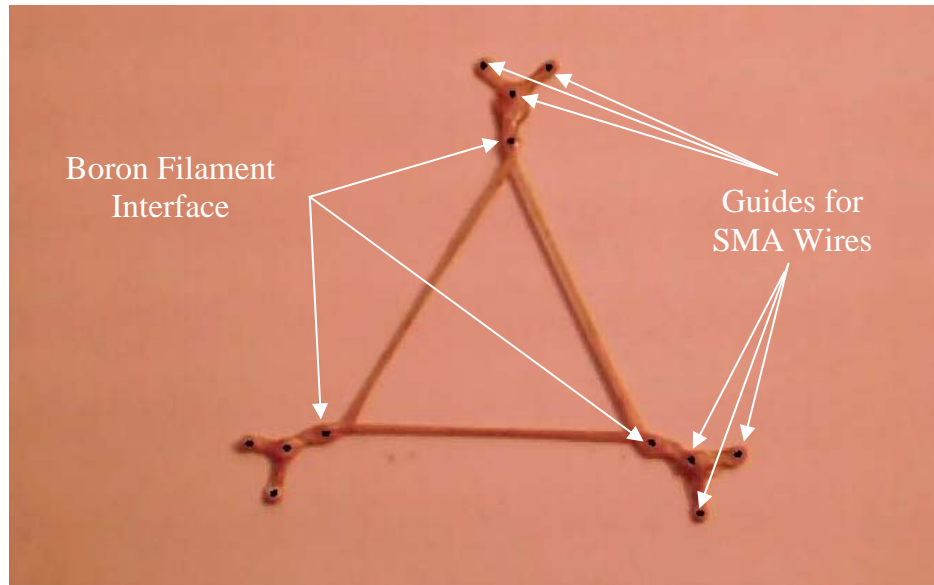
Figure 3.3.2 Enlargement of a Triangular Truss Section to Show the Boron
Filament Interface and Guides for the SMA Wires.
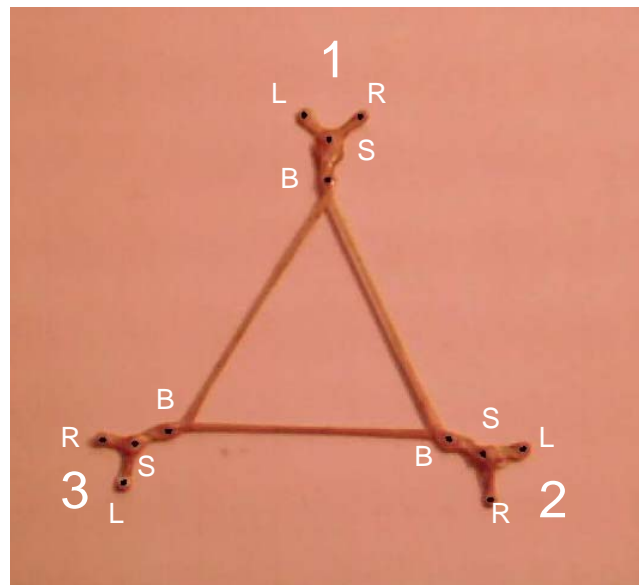
Figure 3.3.3 Triangular Truss Shown With Hole Indexing System.
B Denotes the Boron Interface, *L* Denotes Local Left Upper Hole, *R* Denotes Local
Right Upper Hole, *S* Denotes Shared Hole, and *1,2,* and *3* Denote the Vertex.

3.4 SMA WINDINGS

Three SMA wires were wound helically around the boron-KEVLAR® truss. It is important to note that the strands were parallel so they never touched. The following is a detailed description of the SMA windings using the indexing system.

The first SMA wire started at vertex 1 in the hole L of truss one. Then the same SMA wire passed through the second truss at hole S of vertex 2. Then that SMA wire passed through hole L at vertex 3 of the third truss and so on down the length of the truss. Two other SMA wires started separately at vertex 2 and vertex 3 of truss 1 and continued in a pattern similar to that of the first wire. None of the wires crossed each other or came into contact with the boron. Three opposing SMA wires were similarly strung starting at the other end of the truss. The wires ran through the shared and right holes of the KEVLAR® triangles. The end result was that three SMA wires ran in a clockwise direction three wires ran in a counterclockwise direction without any of the wires crossing.

Opposing pulling wires heated alternately act much like bicep and tricep muscles do to actuate and restore position of an elbow joint. As one muscle (or SMA wire) contracts, the opposing muscle (or SMA wire) extends and vice versa for motion in the opposite direction. For the laboratory test, however, only twisting in only the clockwise direction was tested to prove the basic concept of SMA torsional actuation. The counterclockwise winding would work in an identical manner for actuation in the opposite direction; therefore, testing of the counterclockwise windings was redundant. The redundant wires were left in the truss to show that the opposing wires do not come in contact with the other set of SMA wires.

21

IV. INITIAL DESIGN PHASE TESTING

A truss constructed of four triangular KEVLAR® trusses secured with cyanoacryllate at two inch intervals on three boron filaments as previously described was placed on a test stand. Small sections of brass tubing were crimped at each end of pre-stretched SMA wires to provide a surface to pull against the end of the truss and transfer the force to the truss. Contact wires which had a 0.15 inch diameter were then soldered to the brass crimps. A simple electrical circuit was made with a variable DC power supply, external ammeter used to accurately measure the current, internal voltmeter used to accurately measure the voltage, and SMA wires, which acted as three resistors in parallel. The electrical resistance in the SMA wires provided the heat to the SMA. The electrical supply/control system is shown in Figure 4.1.1.

The truss was attached to the test stand with tape around the top contact wires as in Figure 4.1.2. The straight contact wires naturally resist torsion and would have restrained the actuation of the SMA Truss. Therefore, the contact wires at the bottom of the truss were connected to a torsional strain relief device. The torsional strain relief device was simply a length of the same type of wire used as contact wires which had been coiled into a 0.4 inch diameter. The coiled shape allowed the SMA Truss to deflect more easily.
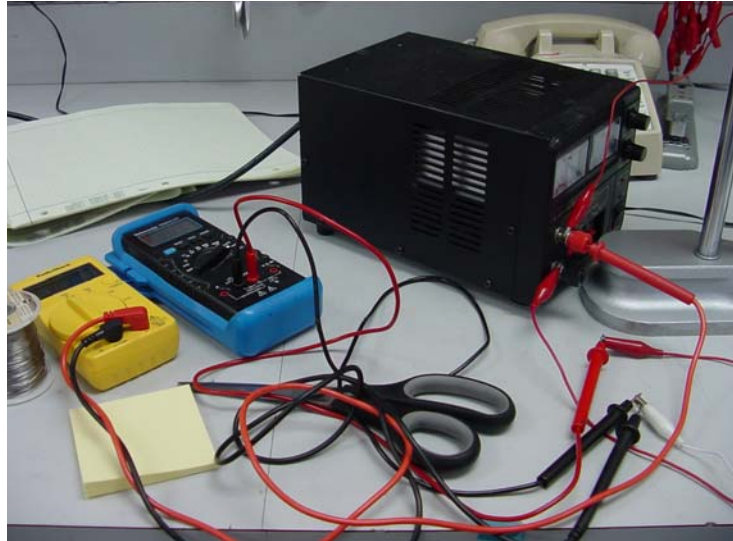
Figure 4.1.1 Photograph of Voltmeter, Ammeter, and DC Power Supply.
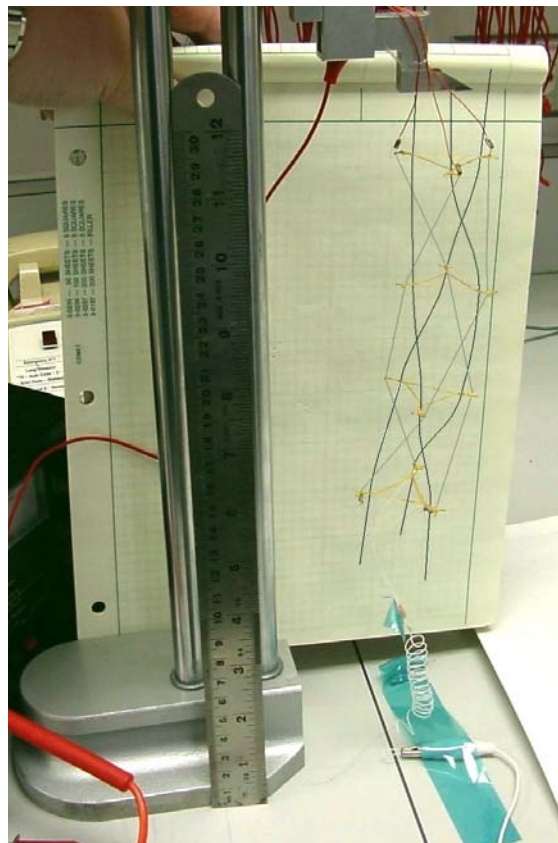
Figure 4.1.2 SMA Truss on Test Stand with Torsional Relief Coil at Bottom

A laser mirror was mounted just above the torsional strain relief. A laser was focused onto the mirror and the reflection from the mirror onto a graph board to measure the deflection as in Figure 4.1.3.
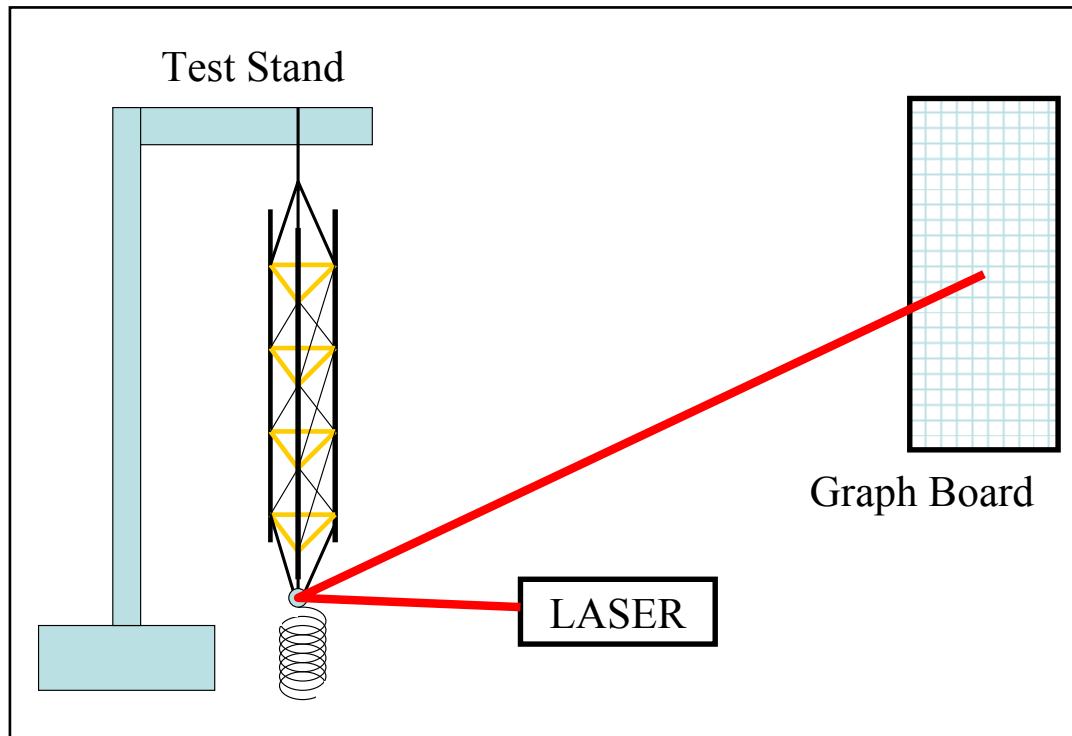
Figure 4.1.3 Diagram of SMA Truss on Test Stand with Laser, Mirror, and Graph Board Measuring Setup.

The focal lengths of the laser and graph board were set such that one inch deflection on the graph board corresponded to one degree of deflection of the truss. The geometry of the reflected laser beam from the deflection mirror is shown in Figure 4.1.4.
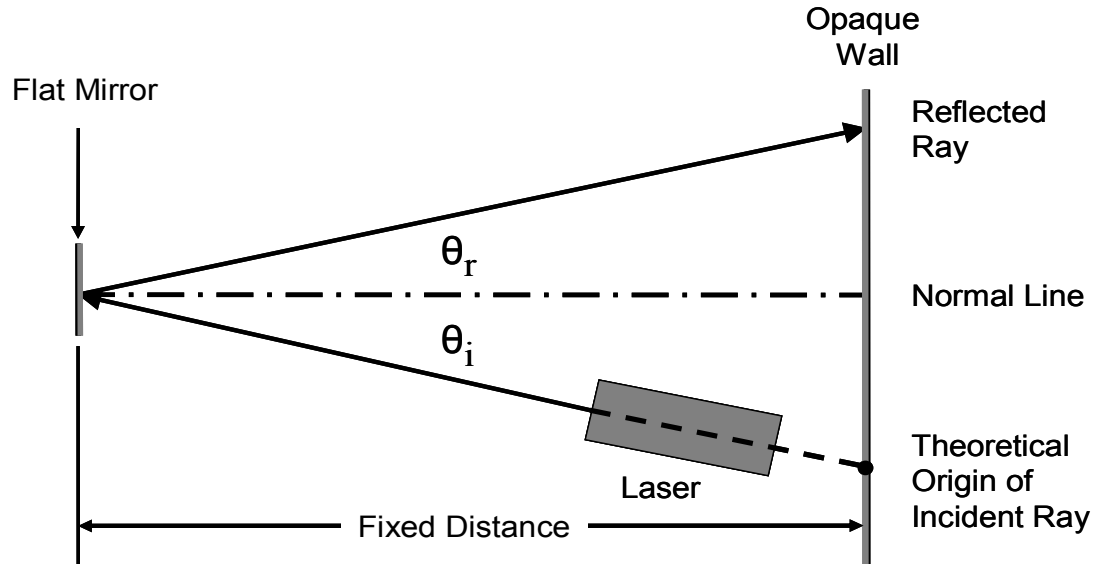
Figure 4.1.4 Diagram of Basic Geometry of Laser Reflection

In Figure 4.1.4, an opaque wall was positioned behind the laser source at a

fixed distance parallel to a flat mirror. The symbol θ_i represents the angle of incidence

between the source laser beam and the normal line to the mirror. The angle of

reflection θ_r is the angle between the normal line to the mirror and the reflected laser

beam from the mirror. The angle of incidence and the angle of reflection are equal

according to the Law of Reflection presented in Equation (2).

$$\theta_r \equiv \theta_i \equiv \theta \qquad\qquad (2)$$

Figure 4.1.5 depicts the same setup as the flat mirror deflects an angle δ.

The perceived angle of deflection on the opaque wall is α.
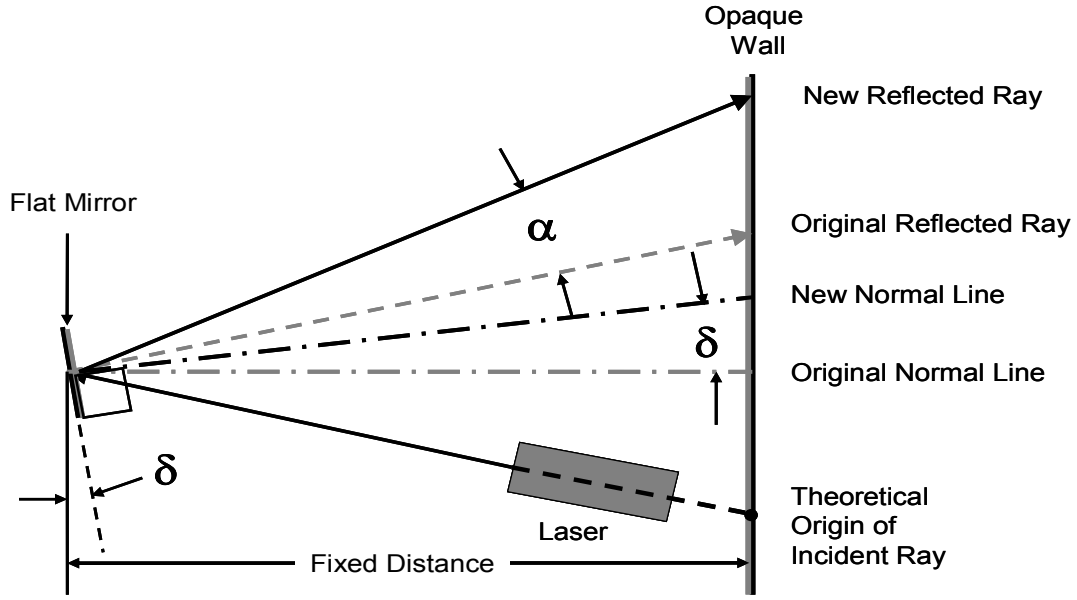
Figure 4.1.5 Diagram of the Geometry Depicting Angular
Deflection of the Beam and Mirror

Since the position of the origin beam stayed fixed relative to the wall, the

perceived angle change α is really the sum of the change in angle of the incident beam

and of the reflected beam from the previous mirror position when the mirror was

parallel to the wall.

$$\alpha = \Delta\theta_i + \Delta\theta_r \qquad (3)$$

Defining the change in angle as the difference between the new angle and old

angle and using the identity from Equation (2) results in Equation (4):

$$\Delta\theta = \theta - \theta_0 \qquad (4)$$

Equation (3) then becomes:

$$\alpha = 2\Delta\theta \qquad (5)$$

Recalling that the mirror deflection is δ and geometric relations for

perpendicular lines, the deflection of the normal line is also δ. The angle δ is also the

true angle of deflection and the change in deflection of the angle of incidence and angle of reflection. Therefore, Equation (5) can be rewritten in terms of δ.

$$\alpha = 2\delta \qquad (6)$$

Since linear distances are more easily measured than angles, angle α is calculated geometrically from the linear displacement of the reflected beam on the opaque wall. Using a fixed distance between the opaque wall and the mirror which is many orders of magnitude larger than the linear displacement, the wall may be assumed to be approximately perpendicular to the original reflected beam. Then the calculation of α becomes simple trigonometry as depicted in Figure 4.1.6.
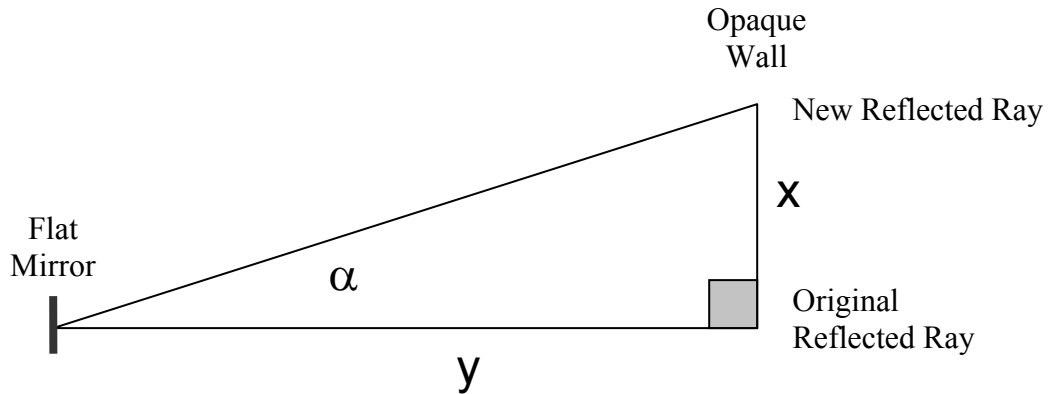
Figure 4.1.6 Depiction of the Perceived Angle Change α with Wall Assumption

The definition for the tangent function of an angle in a right triangle is used to determine angle α. The equation for α is:

$$Tan(\alpha) = \frac{x}{y} \qquad (7)$$

Solving the equation for y, the previous equation becomes:

$$y = \frac{x}{Tan(\alpha)} \qquad (8)$$

27

Realizing that for calculation purposes it would be much easier if δ of 1° corresponds

to x = 1", we let α = 2˚ recalling from Equation (6) that α is twice δ. Plugging in

Equation (8), we get:

$$y = \frac{1"}{Tan(1°)} \approx 28.65" \tag{9}$$

Thus, the experiment used a fixed distance between the mirror and the wall of 28.65"

so that an inch of lateral deflection of the laser beam on the wall corresponded to a 1˚

twist of the truss.

A range of voltages was applied to the circuit, and the current as well as the

angular deflection were measured and recorded. The data was afterward compiled

into a table and plotted. More photographs from the test setup may be found in the

Appendix.

V. INITIAL DESIGN PHASE DATA

The twisting of the SMA truss can be seen qualitatively below in the

photograph. Also presented is a tabulated chart of the data collected in Table 5.1.
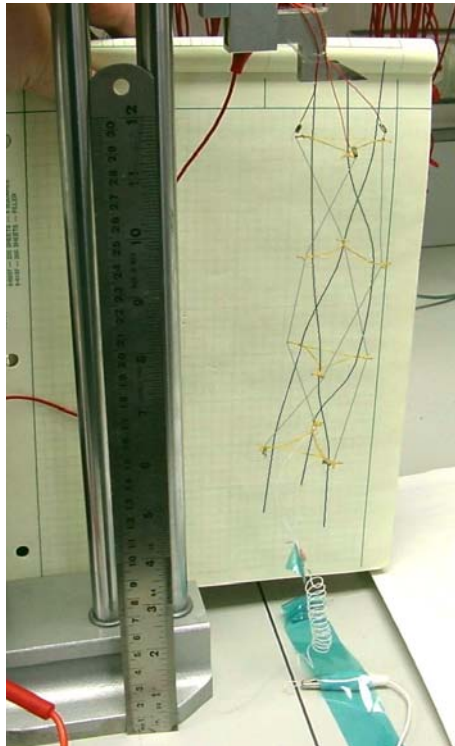
Figure 5.1.1 SMA Truss on Test Stand After Testing.

Table 5.1 Tabulated Data of Voltage With Output Current and Displacement

Voltage	Current	Displacemet (δ)	Voltage	Current	Displacemet (δ)
(mV)	(mA)	(inch)	(mV)	(mA)	(inch)
121	10	0.165	2540	200	-0.276
227	18	0.365	2660	210	-0.843
382	30	0.360	2660	210	-0.692
504	40	0.375	2790	220	-1.184
635	51	0.455	2790	220	-0.572
750	60	0.400	2930	230	-1.543
902	72	0.402	2930	230	-0.956
992	79	0.403	3050	240	-1.882
1130	90	0.385	3050	240	-1.324
1260	100	0.308	3180	250	-3.550
1260	100	0.412	3180	250	-2.083
1380	110	0.302	3170	260	-11.6
1380	110	0.380	3170	260	-11.3
1500	120	0.268	3210	260	-11.6
1500	120	0.371	3210	260	-11.3
1640	131	0.244	3360	270	-12.3
1640	131	0.319	3360	270	-11.4
1770	141	0.152	3400	270	-12.3
1770	141	0.283	3400	270	-11.4
1880	150	0.068	3440	280	-13.9
1880	150	0.194	3440	280	-13.4
2010	160	-0.110	3480	280	-13.9
2010	160	0.137	3480	280	-13.4
2150	170	-0.091	3530	290	-23.4
2150	170	0.089	3530	290	-23.0
2280	180	-0.176	3560	290	-23.4
2280	180	-0.161	3560	290	-23.0
2410	190	-0.464	3610	300	-23.9
2410	190	-0.261	3610	300	-23.1
2540	200	-0.589	3650	300	-23.9

A graph of the Voltage vs. Current of the twisting actuator is provided in
Figure 5.1.2, and a plot of Voltage vs. Deflection of the actuator is presented in Figure
5.1.3.

Figure 5.1.2 Plot of Voltage vs. Current
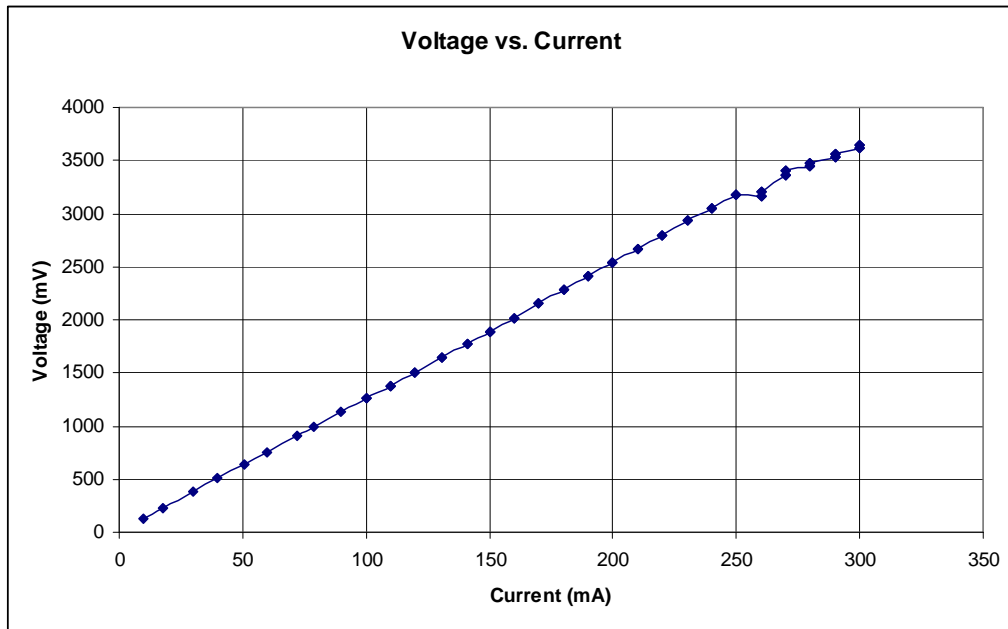
Figure 5.1.3 Plot of Deflection vs. Voltage
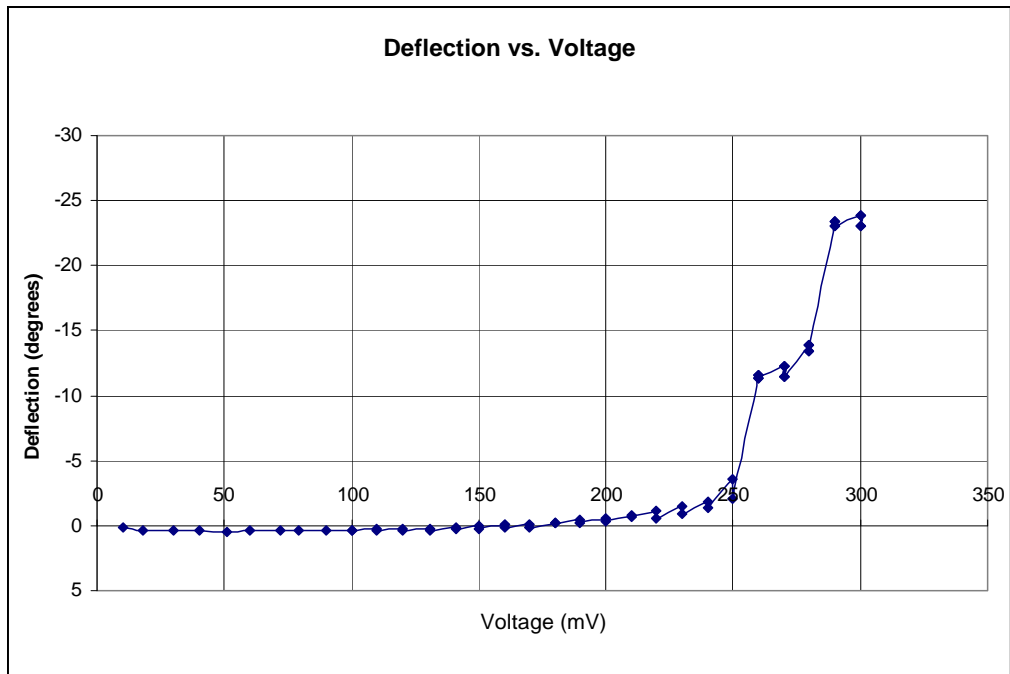
VI. INITIAL DESIGN PHASE CONCLUSIONS

The proof of design SMA Truss actuator performed well during testing and showed that high angular SMA actuation of a truss section is feasible. When heat was applied to the SMA, the SMA caused the truss to twist as is evident qualitatively in Figure 5.1.1. The plot of Voltage vs. Current, Figure 5.1.2, shows a linear relationship between Voltage and Current. Recalling Ohm's law that voltage is current times resistance, the slope of that graph represents the resistance of the system. This is consistent with the published resistance for the type of SMA wire used in this experiment. The maximum angular deflection was approximately twenty-three degrees as shown in the graph of Voltage vs. Deflection, Figure 5.1.3.

SMART met the design requirement that the entire truss twist to accommodate rotational actuation and was an overall success. Since this stage of the design was an intermediate proof of design feature to a more complex design, further testing and development of this particular actuator were abandoned to pursue the integrated actuator. Future recommendations for developing this particular intermediate actuator as its own functional design would include integrating the opposing SMA wires for bi-modal twist and untwist. Also, extensive testing should be performed to determine the fatigue life of the actuator after repeated cycles of twisting. A mathematical model of the twisting actuation would also need to be developed using numerical analysis

methods as the data did not readily converge to any of the 300 closed form solutions which were attempted by using curve fit software. The technological strides and proof of concept discoveries made in the initial design phase directly translated into the success of the final design of the Shape Memory Alloy Robotic Truss.

VII. SECOND DESIGN PHASE

The initial design phase of the SMA Truss actuator demonstrated the capability of a rotationally actuated truss using helically wound SMA actuator wires. The next set of design requirements required the capability of bi-directional actuation, so a new actuator was build which could accommodate bi-directional actuation.

7.1 NEW TRUSS STRUCTURE

Since the small scale of the initial design had made construction tedious and time consuming, the overall scale was increased to facilitate faster prototyping. The new triangular KEVLAR® trusses had exactly the same thickness and orientation of wire guides as the initial design; however the distance between vertices of the new triangles was increased from one inch to two inches and the wire guide hole diameter was increased to accommodate new horizontal members and new 0.005 inch diameter SMA actuator wires. The boron filament horizontal members of the initial design were replaced with 0.05 inch diameter graphite rods due to the limited selection of boron diameters on hand and the hazard of working with boron filaments which are prone to shatter into sharp splinters.

A working prototype truss of 14 inches tall with KEVLAR® triangles fixed with cyanoacryllate at two-inch intervals was constructed and attached firmly to a base

34

of two sheets of 0.16 inch thick modeler's plywood laminated with cyanoacryllate. An end cap was made on the other end of the truss with two laminated pieces of the same modeler's plywood. Both the base and end cap were bored approximately 0.1 inches deep to accept the ends of the graphite rods at right angles. The graphite rods were firmly attached in their holes in the base and end cap with cyanoacryllate.

Since the brass crimping technique in the initial design was difficult to adjust to assure proper pre-tensioning of the SMA wires, a new wire termination system was developed. The new system works much like guitar tuning pegs at the base and anchor screws at the end cap.

Once the wires were properly pretensioned, it was observed that the KEVLAR® trusses buckled under the force of the tightened SMA wires. Plywood triangle webbing was added to the KEVLAR® triangles to carry the compressive load because the trusses buckled during pretensioning of the SMA.
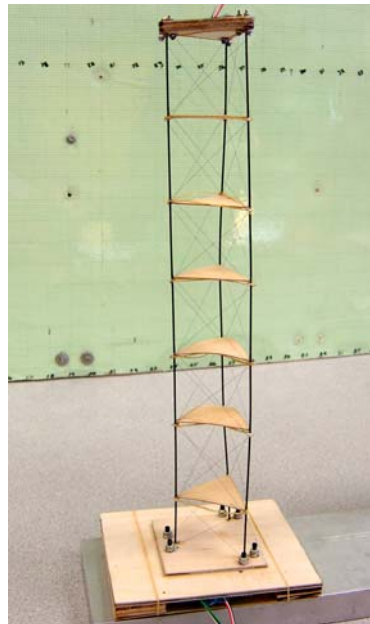
Figure 7.1.1 Photograph of the post buckled Phase Two SMART

7.2 END CAP ASSEMBLY

The end cap assembly consisted of a wooden end cap with anchor screws. Two holes were bored through the end cap at each vertex: one set of holes inside the triangle made by the graphite rods at the vertices and the other set outside that triangle. The six holes had a diameter just larger than a 0-80 size screw and were drilled at an offset angle so they would be accessible to a mini wrench.

The anchor screws were 0-80 size, stainless steel (silver in color), 0.5" long screws with hex heads and a number of #0 stainless steel washers and 0-80 steel nuts. The following is a step by step description of an anchor screw assembly:

1. A piece of 0.005 inch diameter SMA wire was threaded straight through a first size #0 stainless steel washer and a second washer of the same type.

2. The SMA wire was then looped over and threaded in the opposite direction back through the first washer while skipping over the second washer as shown in the following photograph.
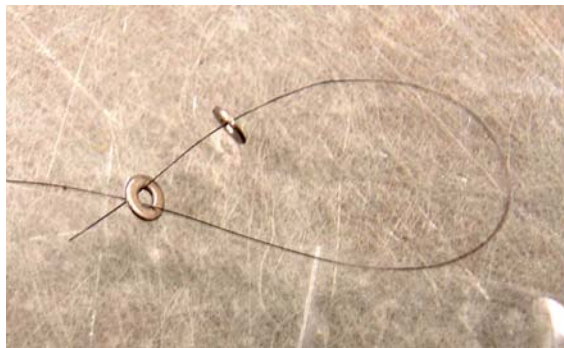
Figure 7.2.1 Photograph of SMA Loop with Washers for Anchoring

3. Then the wire was pulled snug against the washers as shown in the following photograph.
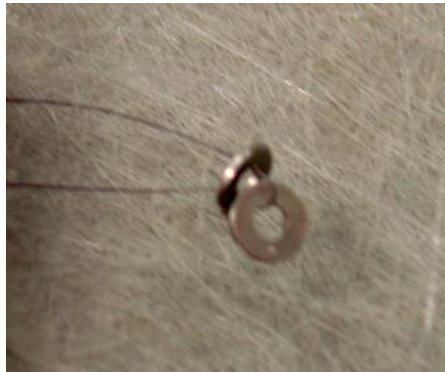
Figure 7.2.2 Photograph of SMA Loop and Washers Tightened

4. The two washers were pressed such that the aligned one on top of the other and a 0-80 size stainless steel screw was pushed through the washers as in Figure 7.2.3.

5. A 0-80 size nut was added to the screw and tightened such that the washers were firmly pressed to the hexagonal head of the screw and to each other. This kept the SMA from being pulled through the washers.

6. Another #0 washer was added to the screw. The screw was inserted into the end cap and another washer was added on the screw at the other side of the end cap.

7. Then one wire of a three-wire cable was stripped of the insulation and wound around the screw on top of the last washer with a 0-80 stainless steel nut tightened firmly down on top of the wire to secure it. Note that no bare wire was left outside of the interface with washer and nut. Refer to Figure 7.2.3.

8. Steps 1-7 were repeated for each of the remaining five anchor screws paying special attention to which wire was attached to which screw obeying the following: Anchor screws on the inside of the triangle were attached to one to each wire of a three-wire cable and the outer anchor screws were attached one to each wire of a separate three-wire cable. Refer to section 7.4 for an explanation of the wiring of the SMA circuit. Below is the completed end cap. See Figure 7.2.3.
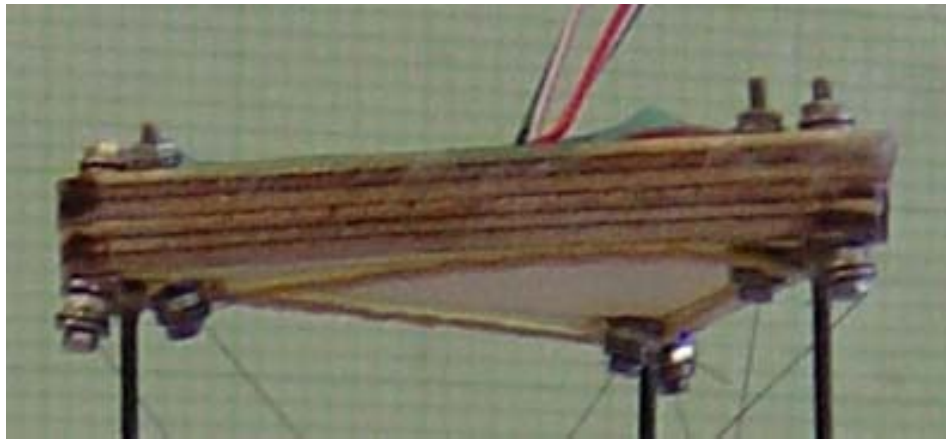
Figure 7.2.3 Photgraph of the Finished End Cap

7.3. BASE PLATE ASSEMBLY

The base plate assembly consisted of the base plate, tensioning screws and wooden feet glued to the base plate which lifted the base plate so that the assembly did not sit on the screws. A wooden cover plate attached with rubber bands to the base plate insured that the ends of the tensioning screws did not come into contact with anything. See Figure 7.3.1.
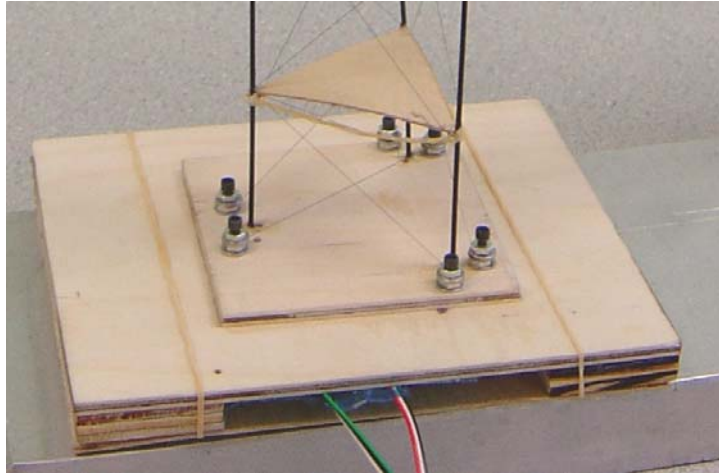
Figure 7.3.1 Close-up Photograph of the Base Plate Assembly

The tensioning screws were 2-56 size, steel alloy (black in color), 0.5" long screws with hex end caps to be used with an Allen wrench. The following is a description of the tensioning screw assembly:

1. A 2-56 sized steel nut followed by two #2 steel washers, another 2-56 steel nut, and a final #2 washer were threaded onto a 2-56 steel alloy screw.

2. The screw assembly was put through a hole in the base plate and another nut was added to the reverse side but not tightened to the base.

3. To attach the SMA, the first two nuts which sandwiched the washers were unscrewed slightly and the SMA was laid between the first two washers.

4. The SMA was wrapped around the screw about four times in the same direction as the helical winding it made with the truss.

5. The two nuts on either side of washers were tightened and the SMA was firmly attached while the screw was free to rotate in its hole in the base.

6. The whole screw was rotated to tension the SMA and then the anchoring nut on the underside was tightened to the base.

7. Then one wire of a three-wire cable was stripped of the insulation and wound around the bottom end of the last nut with another 2-56 steel nut tightened firmly down on top of the wire to secure it. Note that no bare wire was left outside of the interface of nut and nut. Refer to section 7.4 for an explanation of the wiring of the SMA circuit.

7.4 BI-DIRECTIONAL ACTUATION

Both clockwise and counterclockwise windings of 0.005 inch diameter SMA actuator wires were attached to the wire guides of the KEVLAR® trusses. Two separate circuits were made: one with the three clockwise wound SMA wires and the other with the three counterclockwise wound SMA wires. A different tri-wire cable was connected to each set of clockwise or counterclockwise wires at each end. Tri-wire cables which had a green wire in them were connected to the clockwise wound SMAs, and tri-wire cables which had a red wire connected to the counterclockwise wound SMAs. Red insulated alligator-type connecting clips were soldered to each of the cables coming off of the end cap while black alligator-type connectors were soldered to the cables from the base cap.

The black alligator connector of the green (clockwise SMA) cable was connected to the negative terminal of the power supply. The red alligator connector of the green cable was attached to the positive terminal of the power supply. This made a circuit of three resisting SMA wires in parallel as in the initial design. Refer to the section on the initial design for specific circuit setup.

VIII. SECOND DESIGN PHASE TESTING

The second design of the Shape Memory Alloy Robotic Truss was tested to show twisting actuation and opposing twisting actuation of the same truss. Two separate circuits were made. The set of clockwise SMA wires wound around the truss were each attached at the anchor/cap end screws to one strand of a tri-wire cable with a distinguishable green strand. The set of counterclockwise SMA wires wound around the truss were likewise attached individually to a strand in the tri-wire cable with a red strand. The green strand cable from the cap end of the truss (with a soldered red alligator clip) attached mechanically to the positive terminal of a variable voltage power supply. The other green strand cable from the base end of the truss (with a soldered black alligator clip) attached mechanically to the negative terminal of the variable voltage power supply. This created a parallel circuit of three SMA wires acting as resistors. An ammeter internal to the power supply was connected to the circuit in series and measured the input current in the circuit. A voltmeter internal to the power supply was connected in parallel to the circuit to measure the voltage drop of the entire circuit. The second circuit was made similarly by replacing the corresponding alligator clips of the counterclockwise circuit to the same power supply with internal ammeter and voltmeter.

Current was supplied to one circuit at a time to determine the maximum twisting displacement in either direction. When a circuit was connected, current and voltage were turned up in small increments from zero until the ammeter registered and motion was observed. Leaving the power supply set to this current and voltage, the circuits were alternated between clockwise and counter clockwise SMA sets. Then to determine the maximum actuation, the current and voltage were increased by about 20% to increase the speed of actuation and to determine the maximum automated actuation. The circuits were then tested alternately. Finally the circuits were disconnected and the truss was manually twisted to determine the true absolute maximum actuation of the truss itself. The experiment was videotaped and photographed against a background graph board at approximately six inches behind the truss to determine the maximum deflections.

IX. SECOND PHASE DATA

An image from the twist experimental is presented below. Bi-directional actuation was achieved through alternate activation of the clockwise and counterclockwise SMA wire sets. Though the actuation was difficult to measure; it is evident from the video captured and in still images that the truss was capable of at least 60 degrees of twist with a slight preference to the clockwise direction.
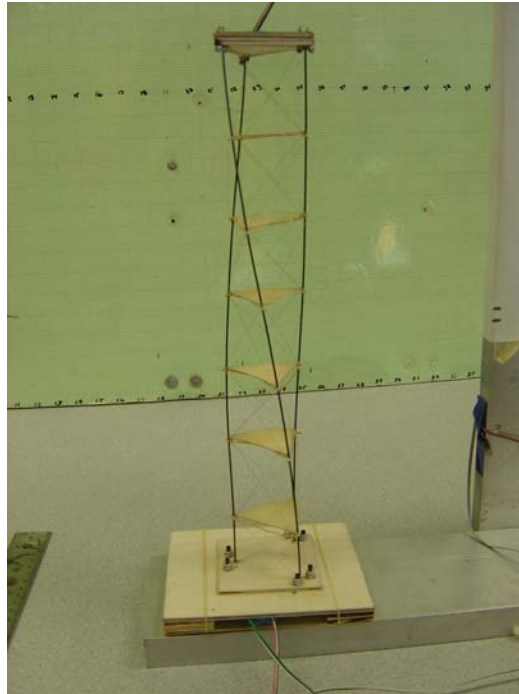
Figure 9.1.1 Photograph of Near Maximum Deflection of the
Second Prototype Twisting Actuator

It was also discovered during testing that there are twisting limits. As the truss twists more, it becomes increasingly difficult to twist the truss further. At higher angles of twist in the truss, the graphite rods which are relatively stiff to twisting

locally in themselves, must twist locally to allow the entire truss to twist. This can be observed in the previous test image. At approximately 180 degrees of rotation, there is also an interference problem with the graphite rods which point touch each other. These conclusions of twist limitations were conducted by manual twisting of the truss structure.

X. SECOND PHASE CONCLUSIONS

The goal of bi-directional actuation was achieved in this design using opposing helical windings of SMA wires. This actuator prototype performed similarly to the previous truss; however, there were some notable conclusions which fell out of the testing. The sizing and stiffness of the rods and fixed ends of the truss affected the amount of actuation achieved. The original triangular trusses of prepreg KEVLAR© were inadequately stiff locally to prevent buckling. This required a redesign of the triangles during testing to add a more a rigid plywood web. Redesign of the SMA carrier triangles was noted as an opportunity for improvement in future prototyping. During testing, it was shown that increasing the voltage and current above minimum operational activation would increase the speed of the actuation; however, it would probably lead to shorter fatigue life. Also, an important observation was made that the more truss module segments in the truss, the more twist actuation is capable because the amount of twist contributed by each truss cell is additive. Because there was discovered a limitation on the amount of twist which can be achieved in this design, a redesign of the support structure was recommended as essential to achieve better twisting capabilities.

XI. THIRD DESIGN PHASE

The third design iteration marked a complete metamorphosis of the design with the resulting third iteration resembling the earlier designs very little; however, the essential technology behind the twisting actuation had changed very little. The third design phase also added bending actuation capability to the twisting truss.

11.1 REDESIGN OF SMART CARRIER STRUCTURE

New consideration was give to the earlier Padget design which had utilized a central graphite rod as a spine with equally spaced KEVLAR® squares with integrated wire guides at the corners and cross members through the center to make a hole through which the spine was placed and secured with cyanoacryllate. The third iteration of SMART utilized Padget's heritage application for a bending actuator with SMA at four corners. Applying the lessons learned from the previous two SMART iterations that KEVLAR® are not sufficiently stiff in compression for more than the smallest scales, the wire guide structure was completely redesigned in a different material. Prepreg fiberglass fabric was chosen as the new material for the SMA wire carriers because of its increased compressive strength as well as for being an electrical insulator.

Instead of using a graphite spine along which the square SMA carriers were permanently affixed with cyanoacryllate, a steel rod of approximately 0.60 inches was

used. Further design influences came from nature and from snake vertebrae which have a great deal of articulation due to the allowed rotation of their vertebrae in the spinal column. Therefore, the fiberglass SMA carriers were allowed to rotate freely about the central steel spine and were only constrained from translating along the spine by the addition of collets on either side of the fiberglass vertebrae. When the first prototype fiberglass vertebrae was produced, it was discovered that it did not slide well about the steel spine because of the "brooming" delaminations which form as holes are drilled; therefore steel washers just larger than the diameter of the steel spine were added as inclusions in the layup to serve as crude bearings. There were no observed delaminations around the modified vertebrae with steel washers for bosses as is evident in the photograph of a finished vertebra. The steel washer bosses also served as alignments for the templates to be affixed to the cured blanks.

Figure 11.1.1 Pattern for Fiberglass Vertebrae, left
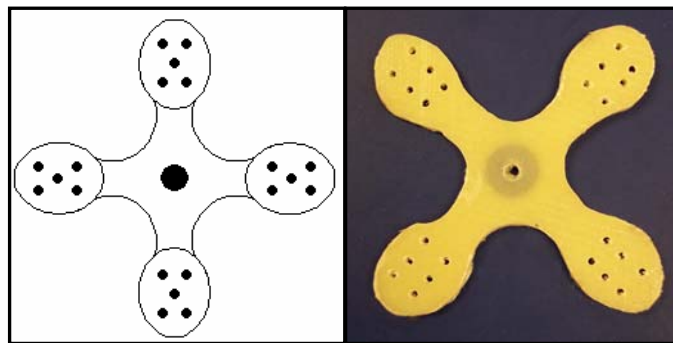and Photograph of Finished Vertebra, right

Further design alterations were made to accommodate six holes for SMA wires in each node instead of the original five. It was thought that by tying the SMA wires to each vertebra that the force would be better transferred to the vertebra instead of relying on contact with the rough drilled hole edge. Also, this method was developed

47

to maximize the pull force of each unit of the spine and allow each vertebra to work equally. This concept was quickly abandoned when it was discovered that the wires degraded rapidly from tying in such tight knots and the heating in the wires was not uniform. The wires located at the ends were doing the most pulling. Rather than remake the vertebrae for only three holes at each corner (one for bending wire, clockwise twist, and counterclockwise twist), the vertebrae were used as is with leaving three of the holes empty. The pull force of the wire was allowed to equivalence itself along the entire length of the spine, and it was discovered that bearing directly on the rough hole guides did not affect the wires significantly. It should be noted as a risk that frequent chafing from the holes could cause premature wear on the SMA wires. The inclusion of some sort of silicone inserts or grommets would alleviate this chafing.

11.2 DETAILED CONSTRUCTION INFORMATION

Two SMARTs were made almost identically except that one was wired for bending and the other for twisting. Both bending and twisting model SMARTs use the same base components as follows:

A. Central Spine
B. Fiberglass Vertebrae
C. Collets
D. End Cap Assembly
E. Anchor Screws
F. Base Assembly
G. Tensioning Screws
H. Shape Memory Alloy (SMA) Wires
I. Electrical wiring

11.3 CENTRAL SPINE

The central spine is a steel rod with a diameter between 0.058 and 0.065 inches. One end of the steel rod is inserted into the base assembly and secured with cyanoacryalate. See Section on Base Assembly. The other end of the rod is sharpened to a point and mates with the End Cap. Refer to section on End Cap Assembly.   See photograph below.
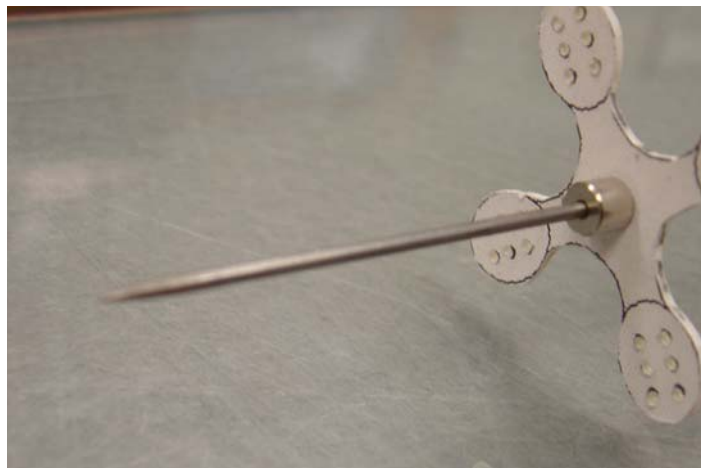
Figure 11.3.1 Cap End of Central Spine

11.4 FIBERGLASS VERTEBRAE

"Clover-shaped" Fiberglass Vertebrae are located every three inches along the Central Spine and simply supported by collets on either side. The individual vertebrae are made from four plies of epoxy pre-impregnated fiberglass with a washer placed middle layer to reinforce the central hole in the finished vertebrae. The blank lay-up is placed between two caul plates and heated in an autoclave for two hours at 177°C. Patterns are placed on the blank to align with the washers. Then the pattern is cut out using a band saw, and the holes are drilled with a hand drill. The holes accommodate

the Shape Memory Alloy wires and act as electrical insulators between the Central

Spine and each SMA wire at the nodes. The Vertebrae slides onto the steel spine and

is secured between two Collets which prevent the vertebrae from translating. See

section 11.5 on collets.
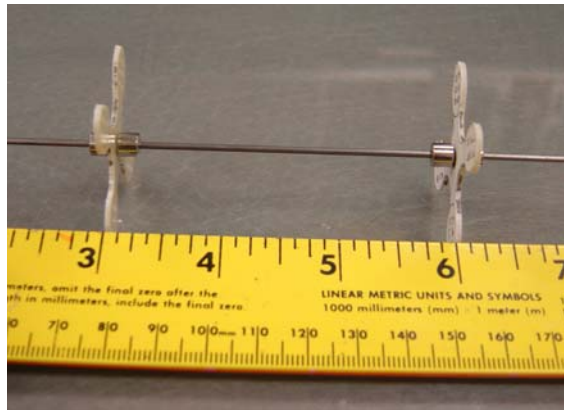
Figure 11.4.1 Integrated Vertebrae on Central Spine

11.5 COLLETS

The Collets are appropriately sized to fit over the steel Central Spine and

contain set screws which tighten them onto the steel spine. The set screws will either

require a jeweler's screwdriver or appropriate sized hex key/Allen key. Collets may

be purchased at a hobby supply store. Each Fiberglass Vertebrae is sandwiched

between two collets to prevent translation up or down the Central Spine. Please note

that the Collets do not prevent rotation.

Figure 11.5.1 Collets against the Fiberglass Vertebrae

11.6 END CAP ASSEMBLY

The End Cap is made up of four components: brass tube stock, tool-hardened steel stub, cap circle, and Anchor Screws. Anchor Screws will be covered in the next section. Brass tubing which just fits over the steel spine is cut to approximately two inches in length. A piece of hardened steel stub which is less than one inch long, conveniently acquired from old drill bits, is chosen with a diameter such that it fits snugly inside the brass tubing. The steel is bonded inside the brass with cyanoacryalate.

Figure 11.6.1 Photograph of the tool-hardened steel stub and brass tubing

51

Next, a piece of "light-ply" hobbiest's plywood with about a 1/8 inch thickness

is cut into a disc with a diameter of approximately two inches. A depression is made

into the center of the disc to accept the brass/steel stub assembly. The brass/steel

assembly is bonded with cyanoacryalate to the End Cap. A filet of cyanoacryalate is

made at the joint to make the connection much stronger. A filet may be made by

applying a cyanoacryalate accelerating spray and cyanoacryalate epoxy in alternating

layers to build up a filet. Holes are drilled for the Anchor Screws according to the

same pattern as the Fiberglass Vertebrae; however, only a single hole is drilled per

pair in the pattern.
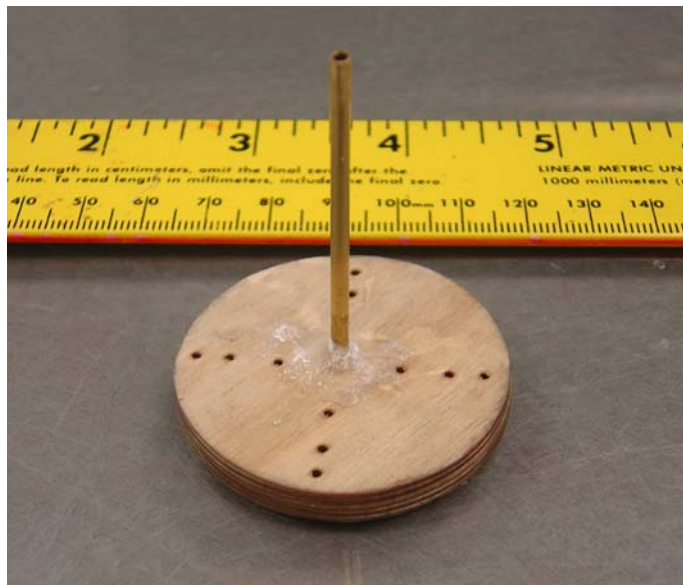
Figure 11.6.2 Photograph of the Finished End Cap Assembly

Graphite lubricating dust, commonly used to lubricate locks and is available in

any hardware store, is put into the brass tubing to allow smooth rotation when the End

Cap Assembly is mounted to the sharpened end of the steel spine. Please note that

because the Steel Spine only contacts the End Cap Assembly at the sharpened point

and graphite lubrication reduces friction, the End Cap Assembly acts like a frictionless bearing and is free to rotate.
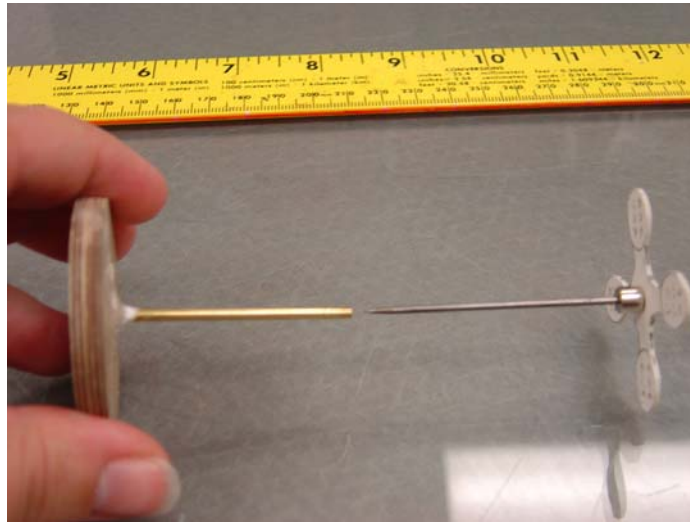
Figure 11.6.3 Photograph of End Cap Mating with End of Central Spine

Please note, the first bending model of S.M.A.R.T. does not have a brass tubing/steel stub on the End Cap Assembly. The end of the Steel Spine simply fit into a hole drilled halfway though the End Cap. This constrains the rotational degree of freedom at the End Cap; however, the bending actuation of the S.M.A.R.T. does not create any torsion on the end. As a result, rotation at the end cap is insignificant for the bending model, and the basic End Cap is sufficient for the Bending S.M.A.R.T.

11.7 ANCHOR SCREWS

The Anchor Screws are the attachment nodes for the Shape Memory Alloy (SMA) wires at the End Cap Assembly. The Anchor Screws are 0-80 steel alloy (black in color) screws that are 1 inch in length and have a hex cap head for use with

an Allen key. The following instructions are the step by step description for installing the Anchor Screws:

1. Take one 0-80 steel alloy (black in color) screw that is 1 inch in length.

2. Thread one 0-80 stainless nut until it is snug against the cap head of the screw. (The original Bender model omitted this step)

3. Take two size #0 stainless steel washers and thread a piece of 0.005 inch diameter SMA wire through both of them.

4. Then loop the SMA wire around the first washer and go though the first washer like in the photograph below:

Figure 11.7.1 Photograph of SMA Loop with Washers for Anchoring

5. Pull the SMA snugly against the washers. See Photograph Below.

Figure 11.7.2 Photograph of SMA Loop and Washers Tightened

6.   Put the 0-80 alloy screw with washer through the washer such that the head of the screw ends up on the same side as the SMA wire ends. See Figure 10.

7.   Push washers up the screw until snug against the nut. See Photograph Below.
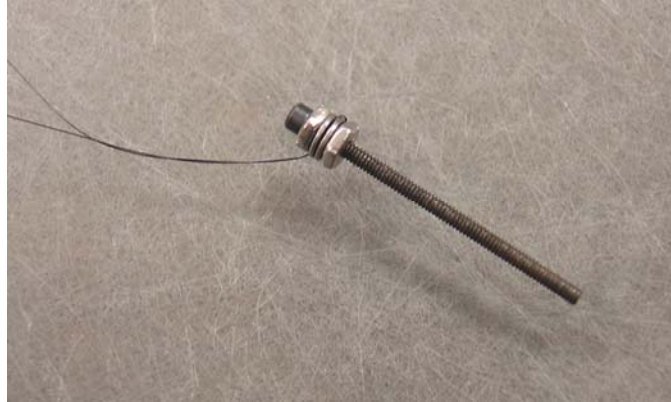
Figure 11.7.3 Anchor Screw with SMA Assembly Attached

8.   Thread another 0-80 stainless nut on the screw until snug against the washers so that the washers are sandwiched between nuts.

9.   Thread another 0-80 stainless nut on the screw and stop before reaching the other nuts/washers leaving approximately a 1/8 inch gap for Bending model S.M.A.R.T., a 1/8 inch gap for Twisting model S.M.A.R.T. outside wires, or a ¼ inch gap for the Twisting model S.M.A.R.T. inner wires.

10.   Add a size #0 stainless steel washer against the last nut on the screw.

11.   Put screw assembly into hole on End Cap and push tight against cap.

12.   Add a size #0 stainless steel washer against the outside facing side of the End Cap.

13.   Add a 0-80 stainless nut until it is snug against washer and End Cap.
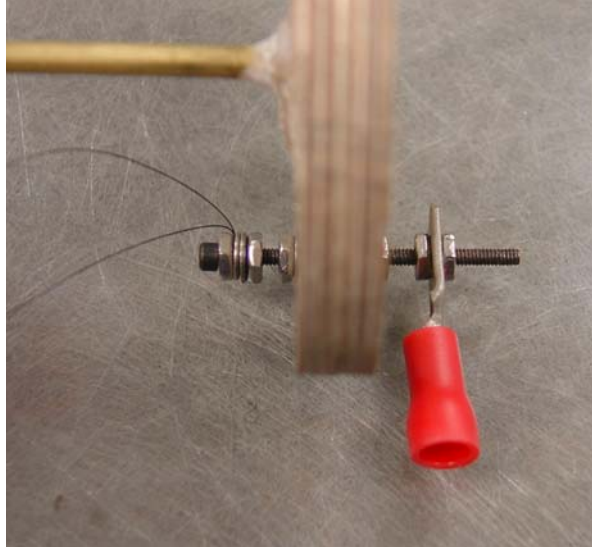
Figure 11.7.4 Completed Anchor Screw Assembly

14.   Check to see that the SMA wire is firmly attached to the screw assembly and that the screw assembly is firmly attached to the End Cap.

15.   For electrical contacts, it may be desirable to add another 0-80 nut to the screw with a 1/8 inch gap. Then add an electrical lead, as pictured above, and secure with another nut. This step may be modified accordingly or omitted as in the case of alligator type electrical connectors.

11.8 BASE ASSEMBLY

The Base Assembly consists of a base block which is about 4 inches long with embedded 2-56 plated nuts for 2-56 steel alloy (black in color) Tension Screws and a Mounting Base Plate. The end of the Central Spine attaches to the Base Assembly in a hole drilled into the top of the block. The joint is secured using cyanoacryalate in the hole and a filet of cyanoacryalate around the outside of the joint. The filet is made

similarly to the filet around the End Cap. A hole is drilled into the base block which is

the diameter of the 2-56 screws at a depth of approximately ¼ inch. Then a punch is

used to make a depression in the wood centered on the screw hole. The nut is placed

in the depression and then pounded into the wood until it is flush with the surface of

the base block. Cyanoacryalate is applied around the edge of the nut to assure the nut

is firmly attached. The process is repeated on each of the four sides of the base as

shown in the following picture.

Figure 11.8.1 Base Assembly Before Ready for Tensioning Screws
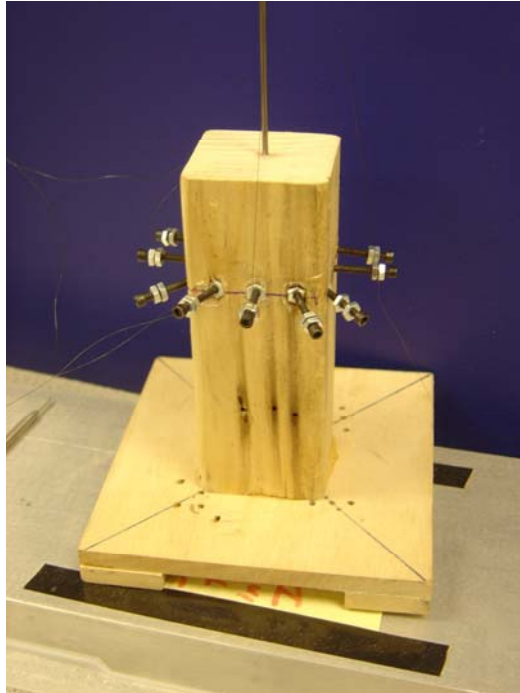
Figure 11.8.2 Finished Base Assembly with Tensioning Screws

11.9 TENSIONING SCREWS

The Tensioning Screws work similar to tuning pegs on a guitar which enable tightening and loosening of wires using a mechanical screw. The Tensioning Screws are made from 2-56 steel alloy (black in color) 1 inch screws.

On the Bending Model, as pictured above in Figure 13, two nuts are screwed together onto the screw with only a slight gap between them. The screw assembly is then turned partially into one of the nuts mounted in the Base Assembly (See Photograph Above). The SMA wire is wound in the gap in a clockwise motion so that as the screw is tightened into the Base Assembly, the wire gets tighter. As the screw is loosened, the wire becomes loose. The SMA must wrap around the screw several

times and the nuts must be tightened together for the SMA wire to be secured

by friction.

The Twisting Model works similarly to the Bending Model with the addition

of two washers between the nuts which give more surface area to clamp onto the

SMA wire.

Tension should be relatively close in each of the wires and may be felt by

touching the wires. The wires should not have any slack but should not be so tight

that the S.M.A.R.T. is almost rigid.

11.10 SHAPE MEMORY ALLOY (SMA) WIRES

Nickel Titanium Shape Memory Alloy Wires with a transition temperature of

70°C and a diameter of 0.005 inches are used. Wires should be cut to approximately

42 inches to insure overrun. Please refer to directions about Anchor screws and

Tensioning Screws for instructions on how to connect the wires.

On the Bending Model, wires run linearly from one node to the next in the

same corresponding hole. On the Twisting Model, sets of wires run clockwise and

counterclockwise as in Figure 11.10.1. The inner set of wires use Teflon tubing

inserted over the wires in the stringing process. The tubing is approximately 2/3 of

the length of the exposed wire length nodes.
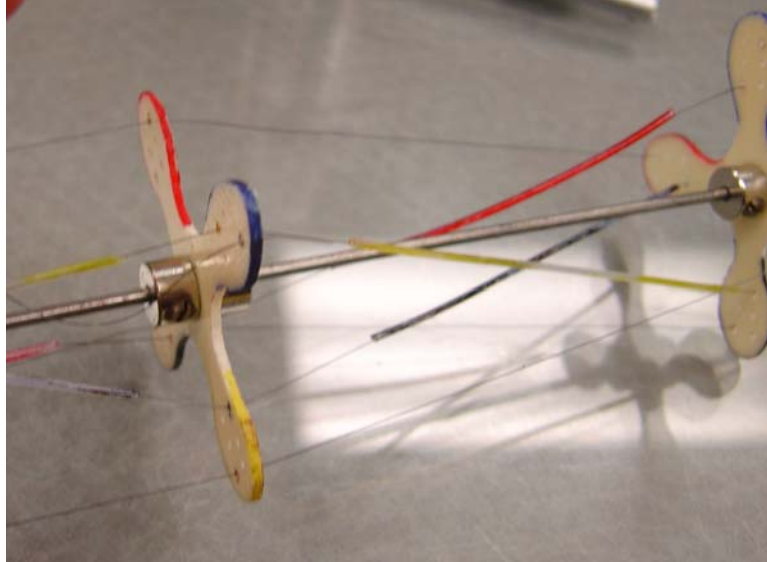
Figure 11.10.1 SMA Wires on the Twisting Model of the SMART

11.11 ELECTRICAL CIRCUIT

Power is supplied to the SMA wires by a manual power supply. Tandem pulling SMA wires are connected in parallel. This means that pairs of wires on the Bending model are wires in parallel, and the four outer wires on the Twisting model are wired in parallel separately from the four inner wires on the Twisting model which are wired together in parallel.

Power Requirements for the S.M.A.R.T.'s are as follows: For the Bending Model, a current not exceeding 1 amp is supplied at a voltage of between 30 and 35 volts. For the Twisting Model, a current not exceeding 1 amp is supplied at a voltage of around 30 volts.

XII. GROUND AND REDUCED GRAVITY FINAL TESTING

The ground based tests of both the twisting and bending were conducted using nearly identical setups as the previous iterations of SMART. The actuation modes were tested separately on identical SMARTs with one wired with helical SMA for twisting and the other wired linearly for bending. This was done to accommodate the need for redundant test articles for two days of testing aboard the NASA C-9 aircraft. If one SMART failed, the other would be ready to go that day and be available for reworking to accommodate the other mode testing during the night between flights. A third truss structure was made; however, it was not wired and was there in case spare parts were needed or could be wired in case both trusses failed or the flown truss could not be reworked.

In ground based testing, SMART was suspended by its base which was clamped in a fixture. A graph board was placed just behind SMART so that displacements could be measured from still and video images taken of the truss. Additionally, a mirror was mounted to the tip of the truss and a laser beam bounced off of the mirror onto a graph board to measure deflections of the tip of SMART more accurately.
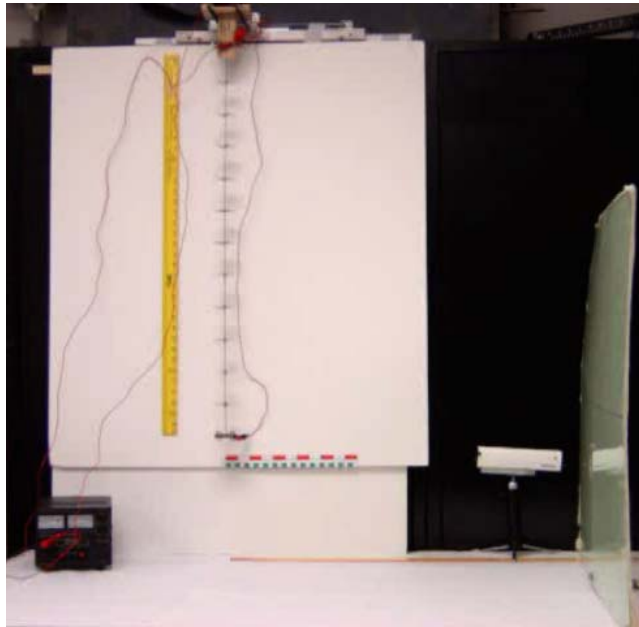
Figure 12.1.1 Ground Based Test Setup of Bending Truss

The phase one design test procedure in Section IV has more details regarding laser

angle/displacement calibration. One inch deflection of the laser beam corresponded to

an upward bend of the truss of approximately one degree of bend in the truss. The

activation current of both SMARTs were found experimentally as before in previous

testing procedures and photographs were taken of the max deflections so that the

defections in the images could be measured. A suspended yardstick served as the

plumb line measurement for the images, and a horizontal scale at the bottom was used

to measure tip directions in the horizontal plane.

The reduced gravity testing aboard the NASA C-9 aircraft tested the bending

actuated SMART both days of flight due to the twisting truss failing in pre-flight

check out and lack of time between flights to rework/rewire the bending to twisting or

the spare. The activation voltage/current was found experimentally in pre-flight

checkout. SMART was suspended from the top of a Plexiglas enclosure and a mirror

was mounted on the tip of SMART to reflect the laser beam onto a graph board. Smart was manually turned on just before the 30 seconds of parabolic path freefall for approximately 60 cycles of parabolas per flight. Digital video equipment continuously captured movements of the reflected laser point as SMART actuated and stored the video to the hard drive of a laptop in the test enclosure. The enclosure was mounted on four large dampers so that vibrations from the C-9 aircraft would have less effect on the data. The detailed circuit, test setup, photographs from the flights, as well as the operations manual for SMART for the reduced gravity testing by the Auburn University NASA Reduced Gravity Student Team is available in the Appendix.

XIII. GROUND AND REDUCED GRAVITY TEST DATA

The two SMARTs were tested in ground based tests. Both SMARTs were slated to fly aboard the NASA C-9 aircraft in reduced gravity; however, due to technical difficulty, the Twisting SMART was scratched and the Bending SMART was flown on both days of flight on March 9-10, 2006 at NASA Johnson in Houston, Texas. The members of the Auburn University team who performed the in flight operations of SMART were Michael Brennison, Ryan Leureck, Megan Brown, and Vanessa Smith, Andrew Wright and Christopher Worley served as ground crew and backup crew for flight operations.

13.1 BENDING SMART GROUND TEST

In testing the bending truss, the laser beam left the graph board before max deflection. Also, because of the high deflection of the tip of SMART, the laser beam no longer focused on the mirror. The still image of bending SMART at maximum actuation shows a tip deflection of 13.5 inches in the horizontal and a tangent angle of the tip section of 58 degrees from the vertical yellow yardstick. Measurements were calculated from image processing of the photograph taken at maximum deflection from a camera mounted perpendicular to test plane.
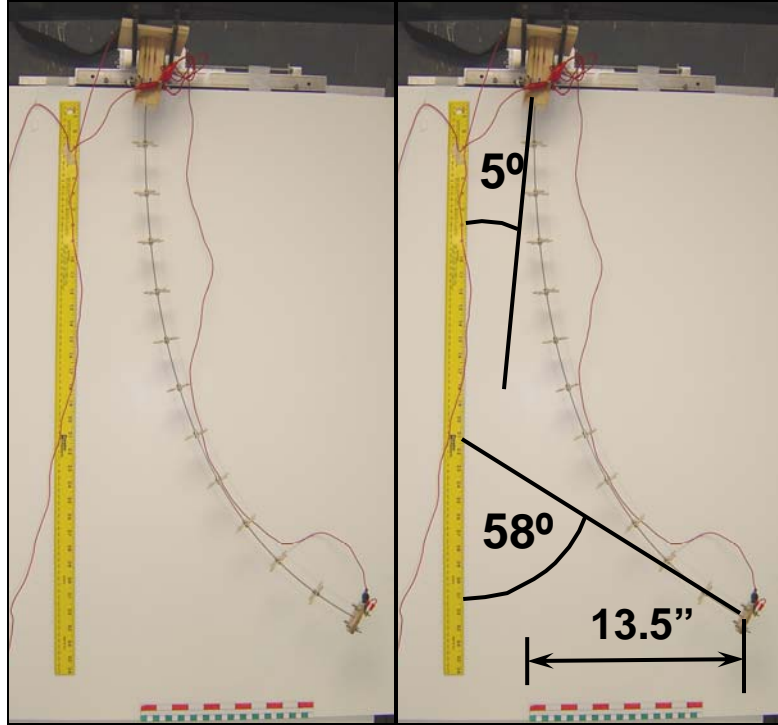
Figure 13.1.1 Photograph of SMART at Maximum Bending Deflection With and Without Displacement Measurements on Image

The base of SMART was observed to rotate in its fixture. Using the same photograph captured at maximum bending deflection, the angle deflected by the base was measured. The 5 ° deflection of the base was added to the tip deflection of 58º which resulted in a total truss deflection of 63º in bending.

Following the bending test, there was an observable post-test residual deformation of the truss. The residual tip deflection was 1.5 inches from pretest and a bending angle residual of 7º. Repeating the test consistently yielded the same deflection and residual post deflection.
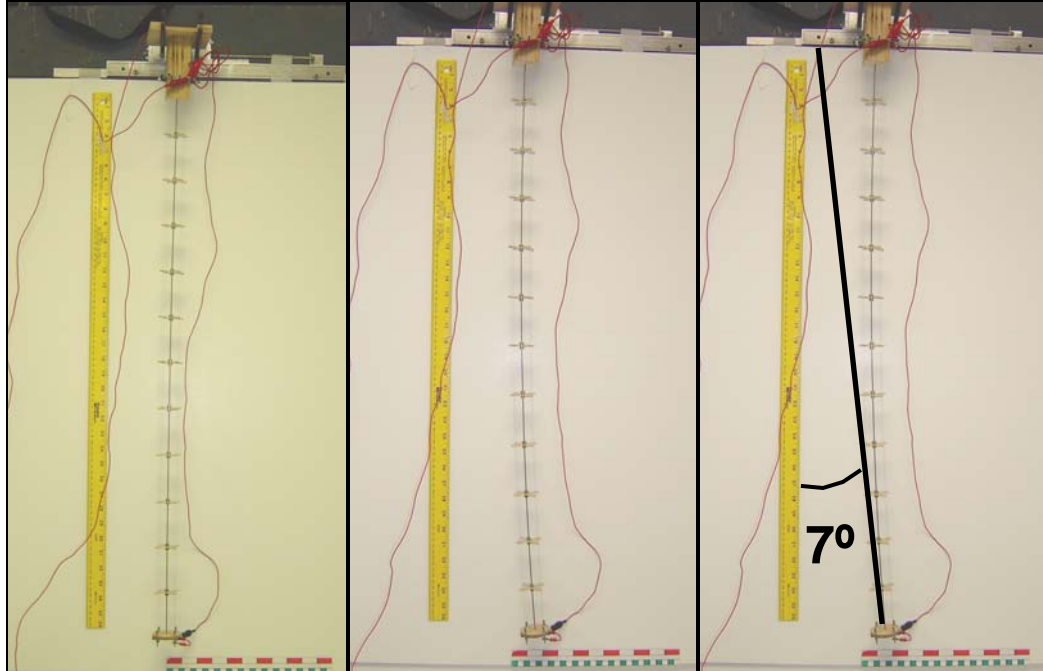
Figure 13.1.2 Side-by-Side Comparisons of Bending SMART Pretest, Posttest, and
Posttest with Residual Bend Measurement

13.2 TWISTING SMART GROUND TEST

The ground based testing of the twisting truss used a mirror mounted on the tip

of the truss in the same setup as the bending test. No appreciable measurements were

captured from the laser point as the point only reflected the local twisting of the end

cap. Local twisting occurred all along the length of the truss, and as a result, the total

deflection of the entire structure was calculated from the measured twisting of each

segment visible at maximum actuation of SMART.

Figure 13.2.1 Photograph of Twisting Truss At Maximum Deflection Posttest.

(Photograph is Rotated 90 Degrees Counterclockwise)
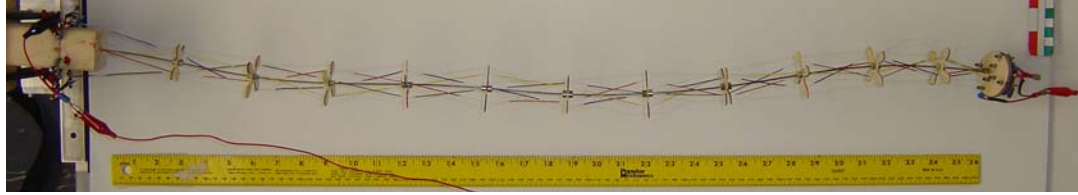
Table 13.2 Twisting of SMART per SEGMENT

Segment	Node From	Node To	Deflection
1	Base	Vertebra 1	0°
2	Vertebra 1	Vertebra 2	75°
3	Vertebra 2	Vertebra 3	15°
4	Vertebra 3	Vertebra 4	45°
5	Vertebra 4	Vertebra 5	45°
6	Vertebra 5	Vertebra 6	30°
7	Vertebra 6	Vertebra 7	90°
8	Vertebra 7	Vertebra 8	75°
9	Vertebra 8	Vertebra 9	90°
10	Vertebra 9	Vertebra 10	90°
11	Vertebra 10	Vertebra 11	90°
12	Vertebra 11	End Cap	90°
TOTAL TWISTING DEFLECTION:			**735°**

Figure 13.2.2 Plot of Twisting of SMART per Segment
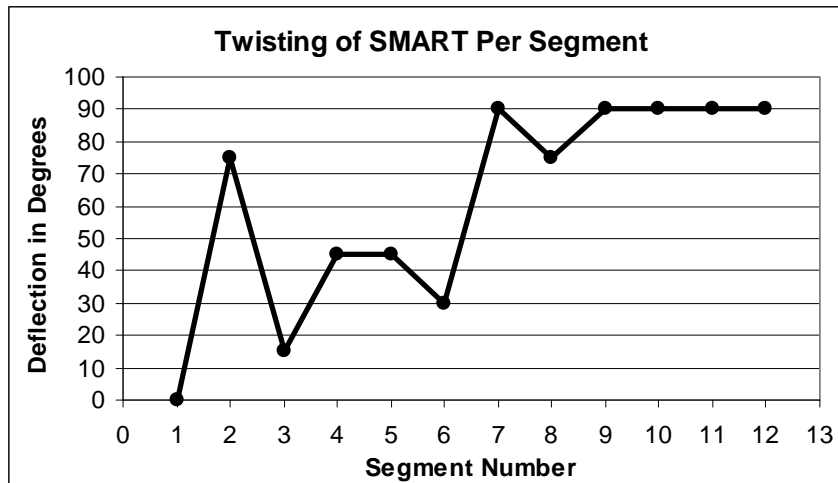
13.3 BENDING SMART REDUCED GRAVITY TEST

The Bending SMART flew aboard the NASA C-9 Aircraft and operated safely.

Post flight analysis of the structure certified that the structure remained intact for the

entire flight and still maintained mechanical functionality following reduced gravity

operations. Observations from the flight test crew indicated that SMART worked as

anticipated and experienced bending deflections of more than 90 degrees during

reduced gravity sets. The video captured in-flight did not have an adequate frame of

reference to measure true deflection of SMART from normal. What can de derived

from the film is that there was a gain of approximately 12 degrees in the max

deflection during the reduced gravity sets when compared to the max deflection in

normal gravity. This was measured from the deflection of the laser beam on a

graphboard between max deflection at constant gravity and max deflection at reduced

gravity.

XIV. SMART PROGRAM CONCLUSIONS

There were many strides as well as many lessons learned over the course of SMART development, and the final SMART design benefits from both. SMART successfully satisfied the fit, form, and function of a degree of deflection bending and twisting actuator. Ground based testing produced approximately 70 degrees bending and a little over 2 full rotations of the structural components. Further reduced gravity testing of SMART in bending resulted in additional bending by conservative estimates of more than 10 degrees. Successful flight tests aboard the NASA C-9 aircraft certified SMART as a reduced gravity actuator and raised the design's technology readiness level one step closer to space operations and the transition from prototype to production.

Further design refinements to be considered in the future are: to find a better method of electrical insulation for SMA wires that will not hinder even heating of the wires, work out actuation control to achieve intermediate actuation, integrating operations of bending and twisting in tandem on a single SMART, creating a mathematical model to further explore the additive effects of segment actuation of a chain of segments, and studying out-gassing of materials in SMART and considering using materials which would be more suitable in a vacuum and under very hot and very cold temperatures.

REFERENCES

1. Fromer, J., *Sectionally Heated Shape Memory Alloy Actuator for Multiple Position Aircraft Roll Control*, M.S. Thesis, Auburn University, Auburn, Alabama, 2002.

2. Srinivasan, A. V., and McFarland, D. M., *Smart Structures: Analysis and Design*, Cambridge University Press, Cambridge, United Kingdom, 2001, pp. 26-72

3. Schwartz, M., *Encyclopedia of Smart Materials,* John Wiley & Sons, Inc., New York, New York, Vol.2, 2002, p. 923.

4. Barrett, R. M., *Introduction to Adaptive Aerostructures*, Short Course Presented at Auburn University, May 2003.

5. Howard, N. A. *Design, Construction, and Analysis of a 2-Degree-Of-Freedom Shape   Memory Alloy Rotary Actuator*, M.S. Thesis, Auburn University, Auburn, Alabama, 2000.

6. Padgett, D. A. *The Design and Construction of a Shape Memory Alloy Tail Boom Actuator.* 41st Aerospace Sciences Meeting and Exhibit. 6-9 January 2003, Reno, Nevada

7. Otsuka, K. and Wayman, C. *Shape Memory Materials*, Cambridge University Press, Cambridge, United Kingdom, 1999.

8. Banks, H., Smith, R., and Wang, Y., *Smart Material Structures: Modeling, Estimation, and Control*, John Wiley & Sons, Inc., New York, New York, 1996, pp. 18-26.

9. Dynalloy Co. Web Page, http://www.sma-inc.com/Actuator.html, 2004.

10. Kelly, A., *Concise Encyclopedia of Composite Materials*, MIT Press, Cambridge, Massachusetts, 1989, pp 33-35.

11. Hibbler, R., *Mechanics of Materials*, Prentice Hall, Upper Saddle River, New Jersey, 2000, p. 92.

APPENDIX A

PROPERTIES OF SHAPE MEMORY ALLOYS

Table A.1 NiTiNOL Flexinol ® Published Technical Data[5]

Flexinol© Technical Data						
Diameter Size (Inches)	Resistance (Ohms/Inch)	Maximum Pull Force (grams)	Approximate* Current at Room Temperature (mA)	Contraction* Time (seconds)	Off Time 70° C Wire** (seconds)	Off Time 90° C Wire** (seconds)
0.001	45	7	20	1	0.1	0.06
0.0015	21	17	30	1	0.25	0.09
0.002	12	35	50	1	0.3	0.1
0.003	5	80	100	1	0.5	0.2
0.004	3	150	180	1	0.8	0.4
0.005	1.8	230	250	1	1.6	0.9
0.006	1.3	330	400	1	2	1.2
0.008	0.8	590	610	1	3.5	2.2
0.01	0.5	930	1000	1	5.5	3.5
0.012	0.33	1250	1750	1	8	6
0.015	0.2	2000	2750	1	13	10
0.02	0.12	3562	4000	1	18	15

Table A.2 Typical Properties of NiTiNOL SMA Alloys[2]

Typical Properties of NiTiNOL Alloys		
Physical Properties		
Melting Point	1300	°C
Density	6.45	g/cm^3
	0.233	lb/in^3
Electrical Resistivity:		
Austenite	~100	$\mu\Omega$cm
Martensite	~70	$\mu\Omega$cm
Thermal Conductivity:		
Austenite	0.18	W/cm°C
Martensite	0.085	W/cm°C
Corrosion Resistance	Similar to 3000 Series Stainless Steel or Ti Alloys	
Mechanical Properties		
Young's Modulus:		
Austenite	~12E6	psi
Martensite	~4.6E6	psi
Yield Strength:		
Austenite	28-100E3	psi
Martensite	10-20E3	psi
Ultimate Strength	130E3	psi
Elongation Failure	20-30	%
Transformation Properties		
Transformation Temperature	-100 to 200	°C
Latent Heat of Transformation	40	cal/g atom
Shape Memory Strain	8.4% Maximum	

APPENDIX B

PHOTOGRAPHS OF TEST SETUP

FOR FIRST DESIGN ITERATION

Figure B.1 Photograph of Test Setup Showing Laser,
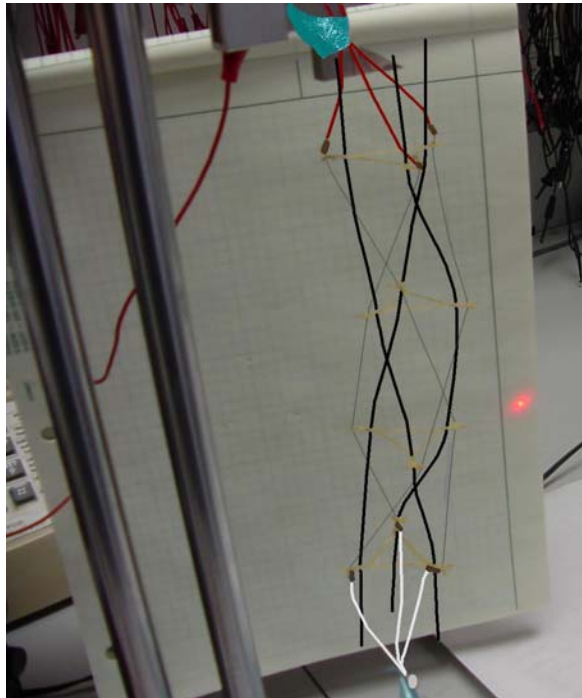Test Stand, and DC Power Supply

Figure B.2 Enhanced photograph of the SMA Truss on the Test Stand. The Dark
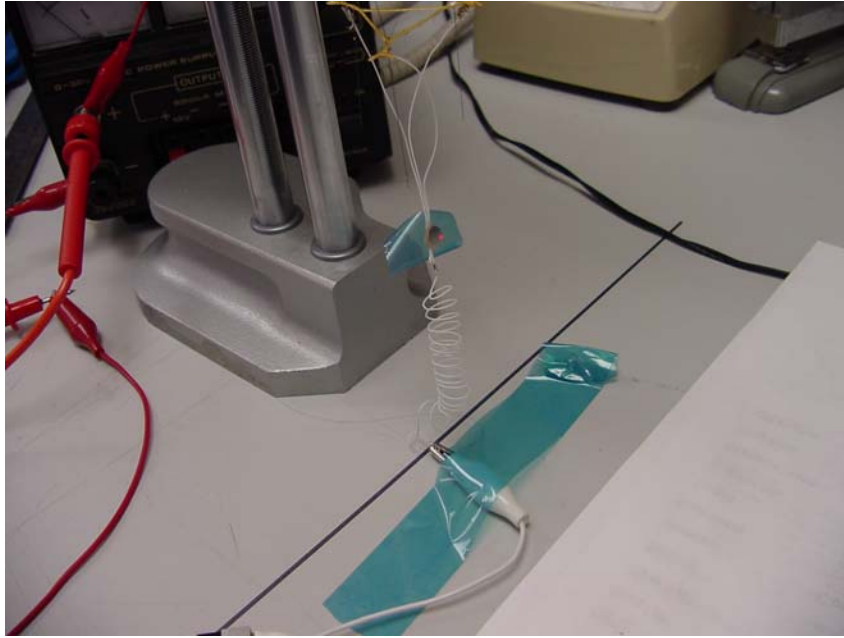Lines Trace the Boron Filaments. The Lighter Gray Lines trace the SMA Wires

Figure B.3 Close-up Photograph of the Torsional Strain Relief Device
Which is the White Coil in the Photograph

Figure B.4 Photograph of Test Setup with Test Stand, Laser, and Wall Graph Board

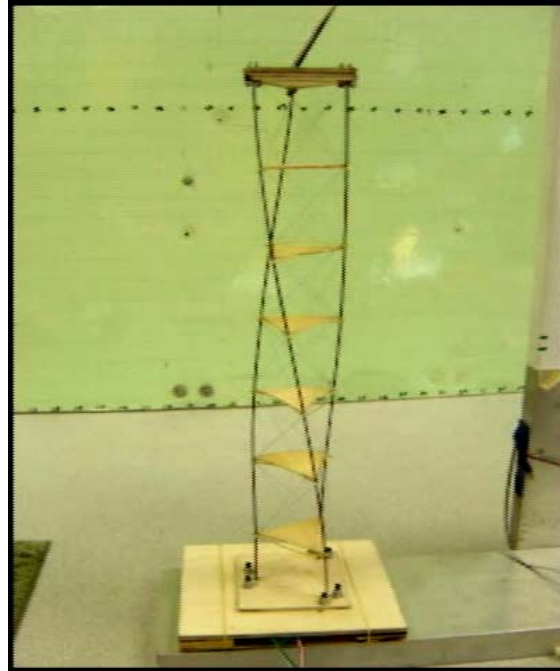APPENDIX C

PHOTOGRAPHS FROM SECOND DESIGN ITERATION

Figure C.1. Frame of Maximum Twist Extracted from
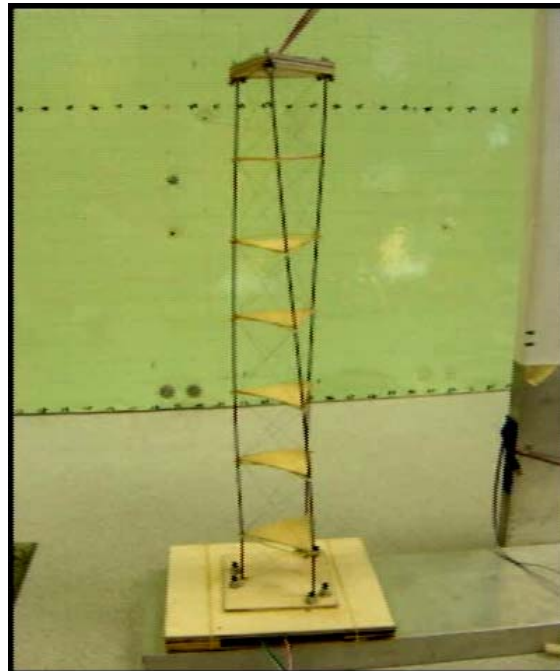Video of Twist in Clockwise Direction.

Figure C.2 Frame of Truss Post Clockwise Twist with Relaxed SMA Extracted from
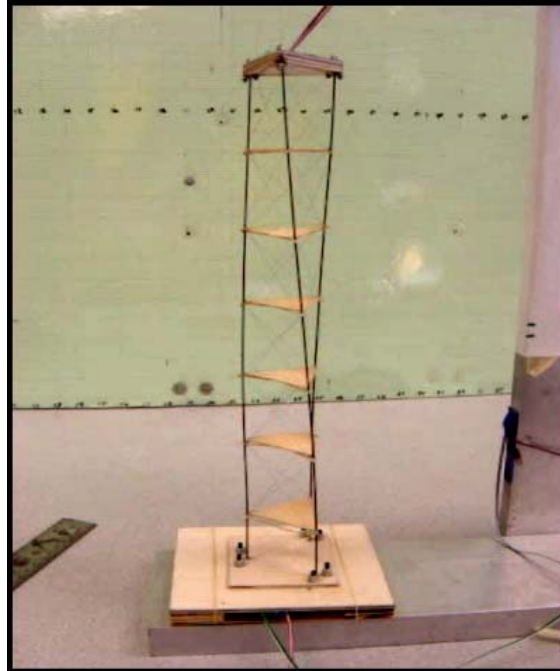Video of Twist in Clockwise Direction. Note the Residual Deformation.

Figure C.3. Frame of Truss at Beginning of Counterclockwise Test Video. Note That This Film Sequence Immediate Follows the Clockwise Test.
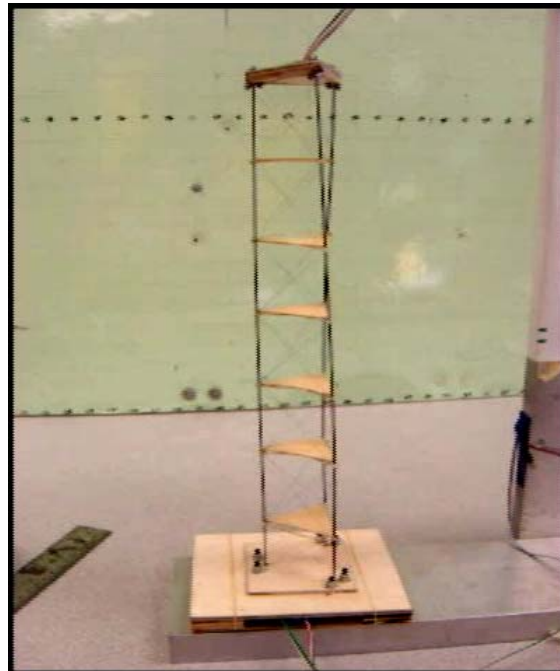

Figure C.4. Frame Extracted Near Maximum Restoring Counterclockwise Twist from Test Video. Note the Buckled Graphite Rods.

APPENDIX D

PHOTOGRAPHS OF POSTTEST
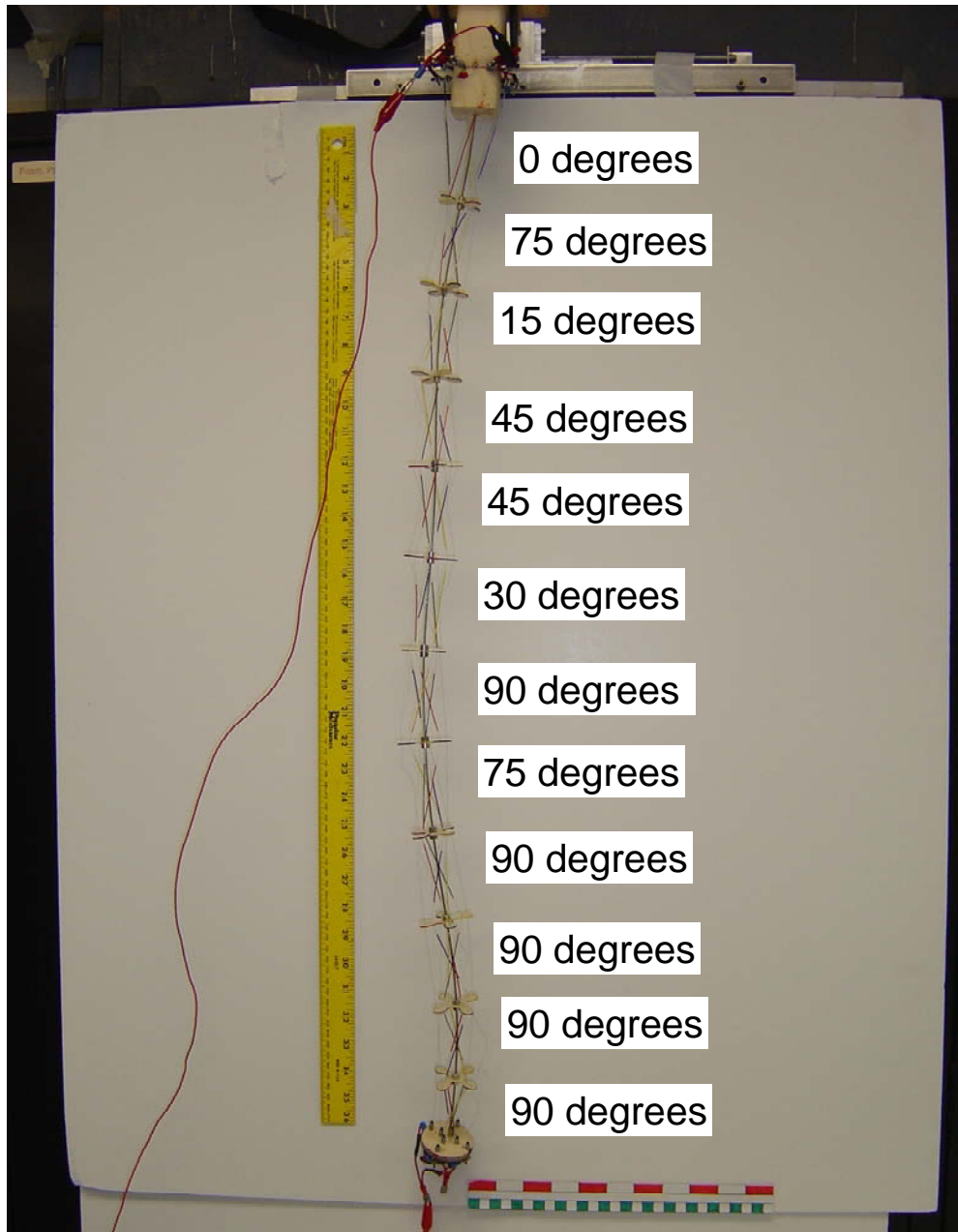
OF FINAL SMART TWISTING TRUSS

Figure D.1. Final Iteration of Twisting Smart Posttest with Measurements of Twist

Note that the nodes were color coded such that at high magnification, one can discern the rotation. Also, several wires fractured in the test, so the degree of twist was likely more than in the posttest photograph.
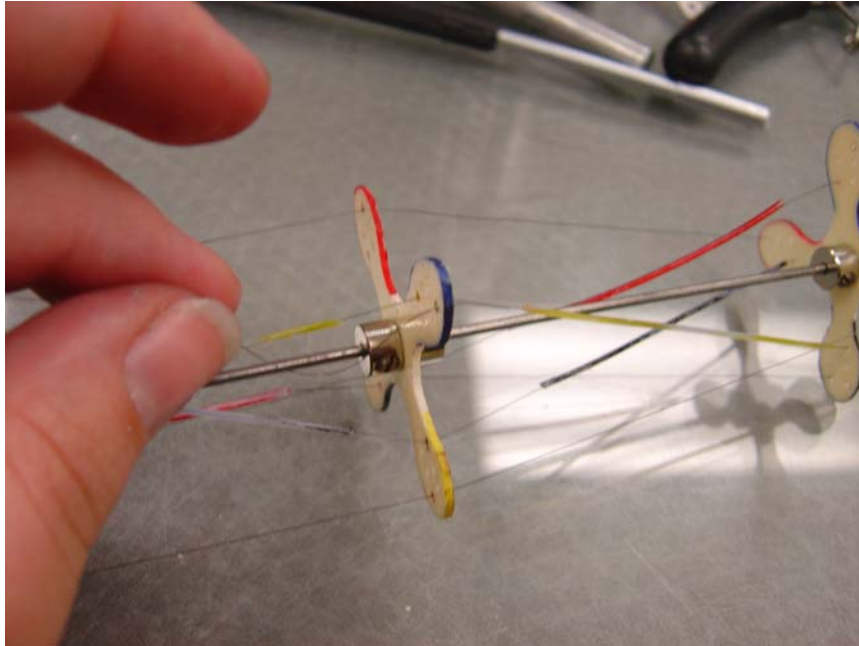
Figure D.2 Close-up Photograph of Twisting SMART with Color Coding Evident

Figure D.3 Researcher Lori Prothero with the Posttest SMART

APPENDIX E

REDUCED GRAVITY TESTING OF SMART IN BENDING

Auburn University
2006
Shape Memory Alloy Robotic Truss
Shape Memory Alloys (SMA) belong to a special class of metals with a unique crystalline structure that can be heat trained to remember a specific size or shape, which it will return to when a heat stimulus is applied. Because of the ability to stretch and shrink repeatedly with strain recovery, SMA are the ideal materials for mechanical devices that perform repetitive tasks, or actuators. An actuator, as the name implies, is a mechanical device which causes something else to move.4 Actuators can be composed of a large number of moving parts such as gears and hydraulic pistons. The light-weight and simplicity of shape memory alloys have made them a great alternative to conventional actuator systems. SMA have the capacity to reduce the complexity of an actuator by replacing many moving parts with a few strands of SMA wire. This reduces spacecraft actuator mass, which can be significant to reducing launch costs. Replacing hydraulic pistons and gears with a single wire also reduces the vibrational settling time, or shaking, as the actuator moves, causing hydraulically mechanized machines to be imprecise in their movements.4 As a result, vibration is a major limiting factor in robotic design, especially in a space environment because it has fewer media to help dampen the undesired movement. Two proof-of-concept designs previously completed by team members show the feasibility of SMA actuation, both linearly and torsionally. The overall goal of Team SMART is to build and test two fully functional SMA actuated Remote Manipulator Systems (RMS's) designed to function in a reduced gravity environment. The team will then compare mechanical characteristics including fatigue life, nodal deflections, total deflections, force, stress, and coiling phenomena between gravitational field and reduced gravity environments. The testing will increase the technological readiness level for SMA spaceflight actuated devices and will help to develop a correlation factor for linear actuation and coiling phenomena.

Figure E.1. Auburn University "Vomit Comet" Team at Team Readiness Review
Team Members (Left to Right): Meghan Brown, Chris Worley, Unknown Girl Not on
Team, Vanessa Smith, Andrew Wright, Ryan Lureck, Michael Brennison

Figure E.2. Team Readiness Review Presentation with SMART Test Module at Right

Figure E.3. Demonstration of SMART Operations Inside Plexiglas Enclosure with
NASA C-9 Aircraft in Background

Figure E.4. Unpacking and Presentation of Twisting SMART at
Team Readiness Review

Figure E.5. Team Preflight Physiological Testing in Altitude Simulator

Figure E.6. Andrew Wright during Physiological Test

Figure E.7. Flight Crew and Flyers from March 9, 2006 at Johnson Space Center in Houston, Texas flight aboard the NASA C-9 Reduced Gravity Aircraft

Figure E.8. Ryan SMART Flyers Leureck and Vanessa Smith from March 9, 2006 Flight

Figure E.9. Andrew Wright, Backup Flyer for SMART Received Opportunity to Fly
with Experiment from Another University on March 9, 2006

Figure E.10. Ryan Leureck During Reduced Gravity Flight on March 9, 2006

Figure E.11. Andrew Wright During Reduced Gravity Flight on March 9, 2006

Figure E.12. Ryan Leureck and Vanessa Smith Operating SMART During Reduced
Gravity Parabola on March 9, 2006

Figure E.13. Vanessa Smith and Ryan Leureck Observing SMART During Reduced Gravity Parabola on March 9, 2006

Figure E.14. Vanessa Smith and Ryan Leureck Observing SMART Through Top of Plexiglass Enclosure on March 9, 2006

Figure E.15. Flight Crew and Flyers from March 10, 2006 at Johnson Space Center in Houston, Texas flight aboard the NASA C-9 Reduced Gravity Aircraft

Figure E.16. Smart Flyers Michael Brennison and Meghan Brown with SMART Test Module on March 10, 2006 Flight

Figure E.17. Smart Flyers Michael Brennison and Meghan Brown During Reduced
Gravity Flight on March 10, 2006

Figure E.18. Meghan Brown During Reduced Gravity on March 10, 2006

Figure E.19. Michael Brennison Checking Computer In Flight on March 10, 2006
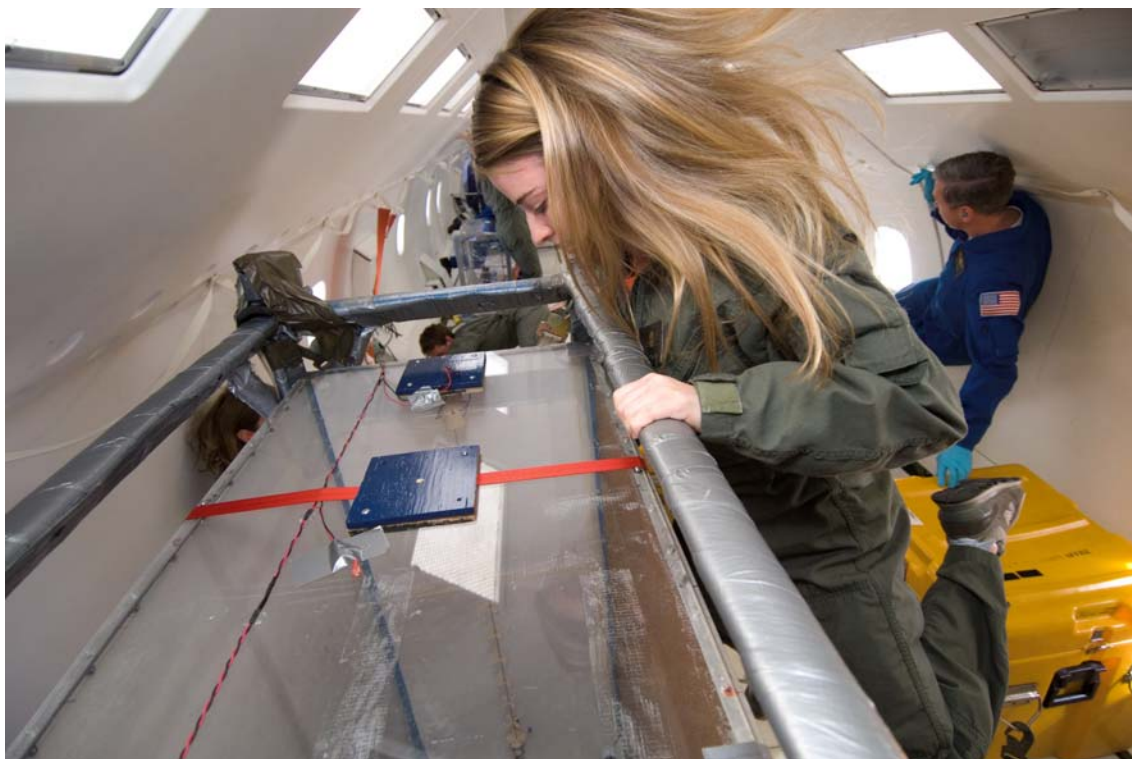

Figure E.20. Meghan Brown Checking SMART Bending Truss Experiment Through Plexiglass Top of Experiment Enclosure on March 10, 2006.